Russian-German Cooperation

Laptev-Sea System

Expedition TRANSDRIFT XV

March 15 - April 28, 2009

CONTENTS

ABBREVIATIONS AND ACRONYMS

AARI	Arctic and Antarctic Research Institute
ADCP	Acoustic Doppler Current Profiler
ASAR	Advanced Synthetic Aperture Radar
AVHRR	Advanced Very High-Resolution Radiometer
AWI	Alfred Wegener Institute for Polar and Marine Research
AWS	Automatic Weather Station
CTD	Conductivity Temperature Depth Meter
ENVISAT	Environmental Satellite of the European Space Agency
GME	Global Model of the German Meteorological Service
IFM-GEOMAR	Leibniz Institute of Marine Sciences
IPY	International Polar Year
IR	Infrared
MODIS	Moderate Resolution Imaging Spectroradiometer
NCEP	National Centers for Environmental Prediction
OSL	Otto Schmidt Laboratory for Polar and Marine Research
SAR	Synthetic Aperture Radar
TIT	Thin ice thickness

THE WINTER EXPEDITION TRANSDRIFT XV TO THE LAPTEV SEA POLYNYA NORTH OF THE LENA DELTA

Over the past decade the Arctic and the adjacent regions have been undergoing significant and sweeping changes. This includes rapidly rising temperatures, shrinking sea-ice cover, destabilization of land-fast ice, increasing coastal erosion due to permafrost degradation, sediment transport by sea ice, and sea-level rise. These changes have clearly manifested themselves in the shelf environments. If they continue, as predicted by climate models, they will have major consequences for the global climate through changes in ocean circulation and circumarctic ecology, as well as implications for human activities. The magnitude of the changes and the mechanisms amplifying or dampening them are still not fully investigated. It is clear, however, that they are essential for modeling and understanding the entire Arctic climate system and its feedbacks for the global system in the future.

The research within the framework of the joint Russian-German project „Laptev Sea System: The Eurasian Shelf Seas in the Arctic's Changing Environment – Frontal Zones and Polynya Systems in the Laptev Sea" has focused both on the ongoing environmental changes, as well as on the understanding of natural variability in the Arctic and, particularly, the Laptev Sea. Polynyas are of major importance for the sea ice production and the ecosystem of the Arctic shelf seas. These polynyas form along the coastline between fast and drift ice and are particularly sensitive to changes in the oceanic and amotspheric circulation. Therefore, they provide a unique object of research into the consequences of these changes for the Arctic.

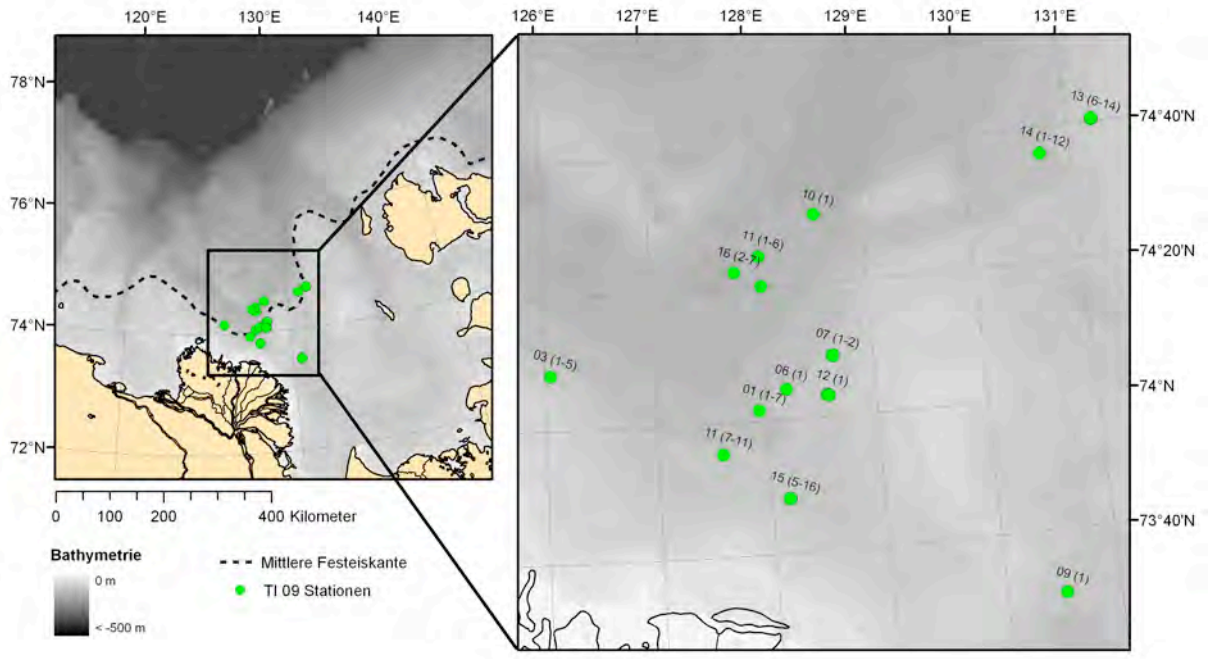

Fig. 1: Station map of the helicopter-based winter expedition TRANSDRIFT XV. The map shows the working area north of the Lena Delta with the stations along the Laptev Sea polynya (black-and-white satellite image).

With the expedition TRANSDRIFT XV we studied the effects of the recent climatic changes on the polynya and frontal systems in the Laptev Sea. For this purpose, four ice camps were installed along the Laptev Sea polynya in order to measure meteorological, oceanographic, hydrochemical, and biological parameters and to study the physical properties of the ice (Fig. 1). Sub-ice bottom stations recorded high-resolution oceanographic parameters during the expedition period in order to provide data on the changes in the water column which are

related to polynya events. At the ice camps as well as close to the coastline north of the Lena Delta, automatic weather stations continuously recorded air temperature, relative humidity, wind speed and direction, atmospheric pressure, and ground pressure.

For the first time we carried out high-resolution measurements of the ice-surface temperature from the transition zone fast ice/polynya/pack ice from a helicopter. These temperature data provide detailed information on the structure of the ice cover and, therefore, a basis for calculating ice-production rates. So far, estimations of this kind were based exclusively on modelling.

The main results of the expedition are the following:

- even slight changes in weather conditions have an impact on the sea-ice production. The sea-ice system of the Arctic is far more sensitive than we supposed;
- the winter of 2008/09 was characterized by a particularly low activity of the Laptev Sea polynya and, therefore, by low ice-production rates;
- Arctic plankton species are increasingly replaced by Atlantic species;
- spring started by a good two weeks earlier than in past years.

With the results of the TRANSDRIFT XIII expedition, of the seafloor observatories which were deployed last year, the data from remote sensing and the various interrelated models, all taken together, we have gained an insight into the mechanisms of the polynya system and their significance for ocean circulation and ice production.

The research team of the expedition comprised 18 scientists from the Alfred Wegener Institute of Polar and Marine Research (AWI), Arctic and Antarctic Research Institute (AARI), Leibniz Institute of Marine Sciences (IFM-GEOMAR), Moscow State University, St. Petersburg State University, State Lena Delta Reserve, and University of Trier. TRANS-DRIFT XV was funded by the Federal Ministry of Education and Research of the Federal Republic of Germany, the Ministry of Science and Education of the Russian Federation and the AARI.

1. Ice surface temperature measurements and photogrammetric sea-ice survey: aerial survey data report

S. Adams[1], T. Krumpen[2], S. Willmes[1], J. Hoelemann[2], A. Helbig[1]
[1]Trier University, Faculty of Geography / Geosciences, Dept. of Environmental Meteorology, Trier, Germany
[2]Alfred Wegener Institute for Polar and Marine Research, Bremerhaven, Germany

1.1. Introduction

The Laptev Sea polynya represents an area of significant net ice production in the Arctic. For the quantification of ice production by means of remote sensing, the investigation of the thin ice thickness (TIT) distribution within the polynya is essential. Therefore, profile flights across the polynya including measurements of the ice surface temperature with very high spatial resolution and a photogrammetric sea-ice survey were performed. The ice surface temperature profiles will be used to retrieve the TIT with the modified thermal ice thickness algorithm developed by Yu and Rothrock (1996). This analysis will result in a validation of thermal ice thickness retrieved from MODIS/AVHRR ice surface temperature. Moreover, we will investigate the development of the ice thickness within the polynya over the same profiles. The aerial pictures give an overview of the general ice conditions.

Here we present all tracks/profiles acquired during the TRANSDRIFT XV expedition.

1.2. Flight operation

The aerial survey includes measurements of the ice surface temperature with the KT 15 II P (KT15) and the photogrammetric sea-ice imagery. All the profile flights across the polynya were operated by T. Krumpen, S. Adams, J. Hoelemann and A. Helbig.

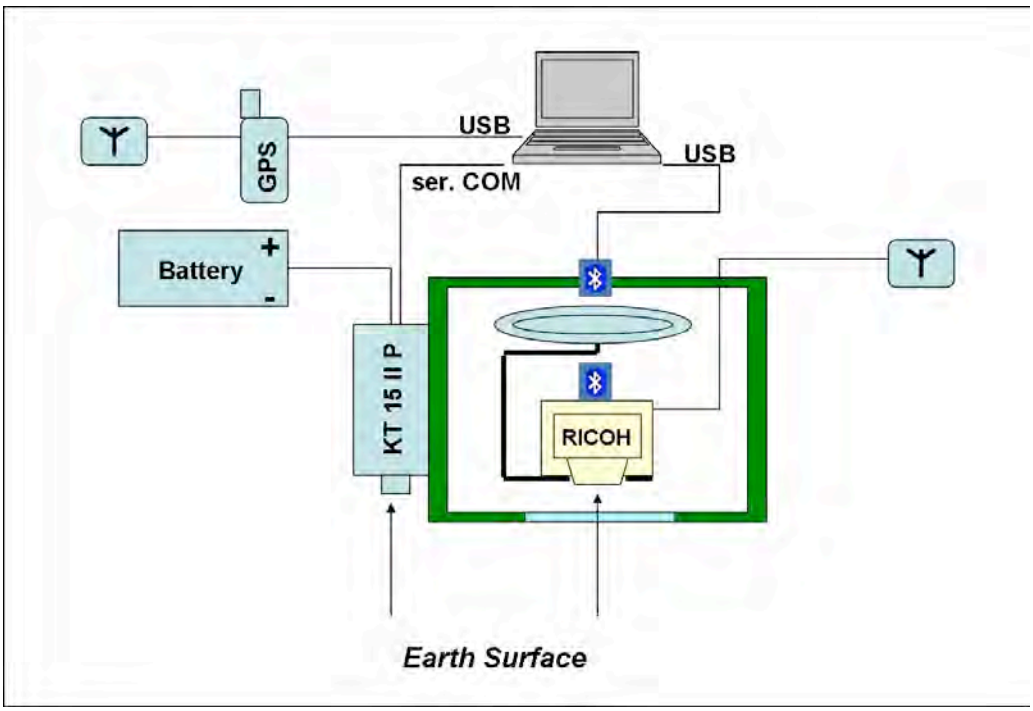

Fig. 3: Measurement system in the helicopter; the green box is fixed in the helicopter hatch.

The measurement system (Fig. 3) includes the KT15 and a RICOH digital camera. The digital camera is equipped with a 1Hz-GPS, which is used together with a second external 1Hz-GPS for geolocation of the ice surface temperature measurements and the aerial photographs. After

the installation of the measurement system in the helicopter (approx. 40 min), across-polynya data were acquired starting from the current field station on the sea ice. Start and end node, the turning points and the track length were chosen according to 1. the operating area of other work packages, 2. available fuel capacity, 3. weather conditions, and 4. ice conditions. In total 9 profiles were taken between March 24 and April 21, 2009. The flight time amounted to roughly 9 hours. The average flight altitude was 100 m and the average flight speed of the helicopter was 120 km/h.

The radiation pyrometer KT 15 II P (HEITRONICS Infrarot Messtechnik GmbH Wiesbaden) is used for measuring the surface temperature of open water, ice and snow. The emitted long-wave radiation of the surfaces is detected in the wavelength range of 9.0 to 11.5 µm. Within this wavelength range the influence of atmospheric gases (especially water vapour and CO_2) is very low, thus the flight altitude is not important for the accuracy of the measurement results. The device provides temperature values considering an arbitrary emission coefficient between $\varepsilon = 0$ and 1. For all measurements we chose an emission coefficient of 1.0. It is also possible to apply a specific emission coefficient, e.g. for ice $\varepsilon = 0.997$ during analysis. The measurement range of the device spans -50 to 200°C. The spatial resolution is 4 m at 100 m flight altitude. Hence, the detected area is significantly smaller compared with the digital camera frames (120 m x 80 m). The setting time is 1 s. Over a serial port the temperature values were transferred to a computer. The software EasyMeas was used for data logging and real-time plotting, which guaranteed a continuous control during flight operations.

1.3. Activities

All activities related to the KT15 ice surface temperature profiling and the photogrammetric sea-ice survey are highlighted in Figure 4. Tracks were taken from the fast ice edge towards a pre-defined point of return and back.

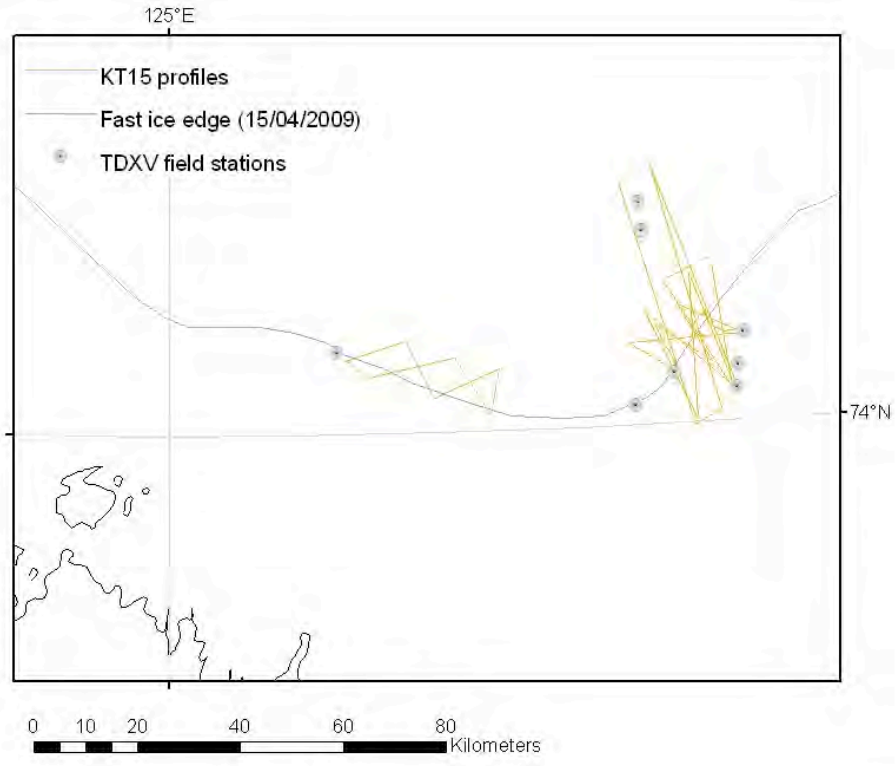

Fig. 4: KT15 flights between March 24 and April 21, 2009.

1.3.1. KT15 tracks

The flight tracks cover the polynya from 74.01°N and 74.43°N and from 127.91°E to 128.64°E (West New Siberian Polynya). The flight track, started from station TI09-3 on March 26, 2009, covers the polynya further west from 74.01°N to 74.15°N and from 126.10°E to 127.06°E. Individual profiles are presented in Chapter 1.4. Table 1 lists a short description of all the flights which were taken between March 24 and April 21, 2009.

Table 1: List of all KT15 tracks

Profile ID	Station	Comment
20090324	TI09-1	Only short profile over the polynya due to the calibration of the aerial photos, instrument breakdown after calibration flight
20090326	TI09-3	Approx. 85 km profile, crossing the polynya 6 times
20090327	TI09-4	Approx. 85 km profile, crossing the polynya 6 times
20090401	TI09-5	Approx. 15 km profile, crossing the polynya once
20090408	TI09-8	Approx. 100 km profile, crossing the polynya 4 times
20090414	TI09-10	Profile from 20090408 is repeated
20090415	TI09-11	Approx. 150 km profile, crossing the polynya 3 times, TerraSAR frame (20090415, 08:37 UTC)
20090421	TI09-13, 14	Approx. 60 km profile, crossing the polynya twice, and short reference profile on thin ice (~15 cm), slow flight twice over this profile

1.3.2. Ground truthing

A reference profile of ice thicknesses was measured at station TI09-14 on April 21, 2009. A thin ice floe in proximity to the fast ice edge was chosen to measure a 250 m profile of ice thickness at 12 drill holes (Fig. 5).

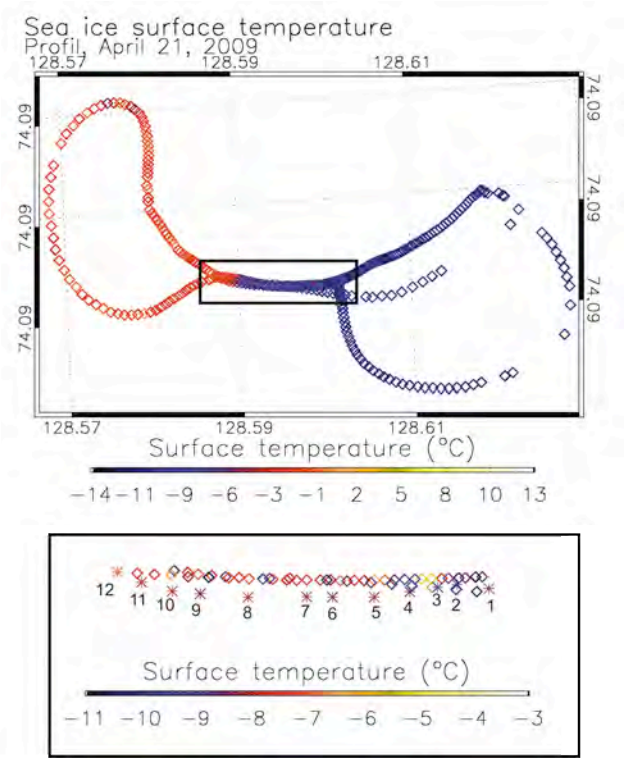

Fig. 5: (a) KT15 profile on April 21, 2009 (TI09-14), black box: area where ice thickness was measured; (b) extract of profile TI09-14, diamonds: position of KT15 measurement points, stars mark the position of Omega-scope measurement points and the ice holes, the colors show the ice surface temperature (Table 2).

On this profile the ice thickness varied between 15 and 22 cm. In addition to the ice thickness, surface temperature was measured with the IR Thermometer Omegascope Model OS71 (Omegascope) handheld with a distance of 50 cm to the ground and without snow cover. Near the measurement points 8 to 12 frost flowers were present on top of the ice, therefore both the surface temperature of the frost patterns and ice without snow cover was measured to investigate the temperature difference of the surface types.

Table 2: Measured ice thickness and ice temperature and, where available, the frost pattern surface temperature T_s measured with Omegascope for the 12 ice holes depicted in Figure 3.

Hole	Ice thickness [cm]	T, over ice [°C]	T, over frost flowers [°C]
1	15.0	-8.1	N.A.
2	16.0	-10.0	N.A.
3	15.5	-9.0	N.A.
4	15.0	-8.2	N.A.
5	19.0	-8.0	N.A.
6	20.0	-8.2	N.A.
7	20.5	-8.0	N.A.
8	15.0	-7.8	-8.8
9	20.5	-8.2	-8.8
10	14.5	-7.5	-9.0
11	22.0	-7.8	-8.8
12	18.0	-7.0	-8.7

1.3.3. Photogrammetric survey

During all flights, nadir-looking sea-ice photographs were taken. The average spatial coverage is 120 m x 80 m. The temporal coverage is at least 30 sec. The images give an overview of the ice conditions during the aerial survey. In addition they will be used to validate the derived TIT from KT15 ice surface temperature measurements, as well as to support ENVISAT-SAR and TerraSAR X image interpretation and for the derivation of an approximate albedo profile, which is necessary for the inversion from the surface temperature to TIT.

Figure 6 demonstrates the different ice conditions across the polynya with aerial imagery for selected positions. Next to the fast ice edge open water with frazil ice streaks was found (image 1). Moving further north the area of open water decreases and the streaks of frazil ice grow wider (image 2). Image 3 shows a thin ice sheet, small consolidated floes and some brash ice. Partly rafted and very thin ice is observed at position 4. Ice thickness and rafting increase further off-shore until position 6. Rafting and small patches of open water are shown in image 5. At position 7 a closed ice cover is observed.

1.4. Processing

1.4.1. Basic principle

We will use the KT15 ice surface temperature measurements for validation of thermal ice thickness derived from infrared satellite data and for the investigation of thin ice development within the polynya. In contrast to satellite data the airborne data has a spatial resolution of approximately 4 m, which is unprecedented in terms of deriving TIT.

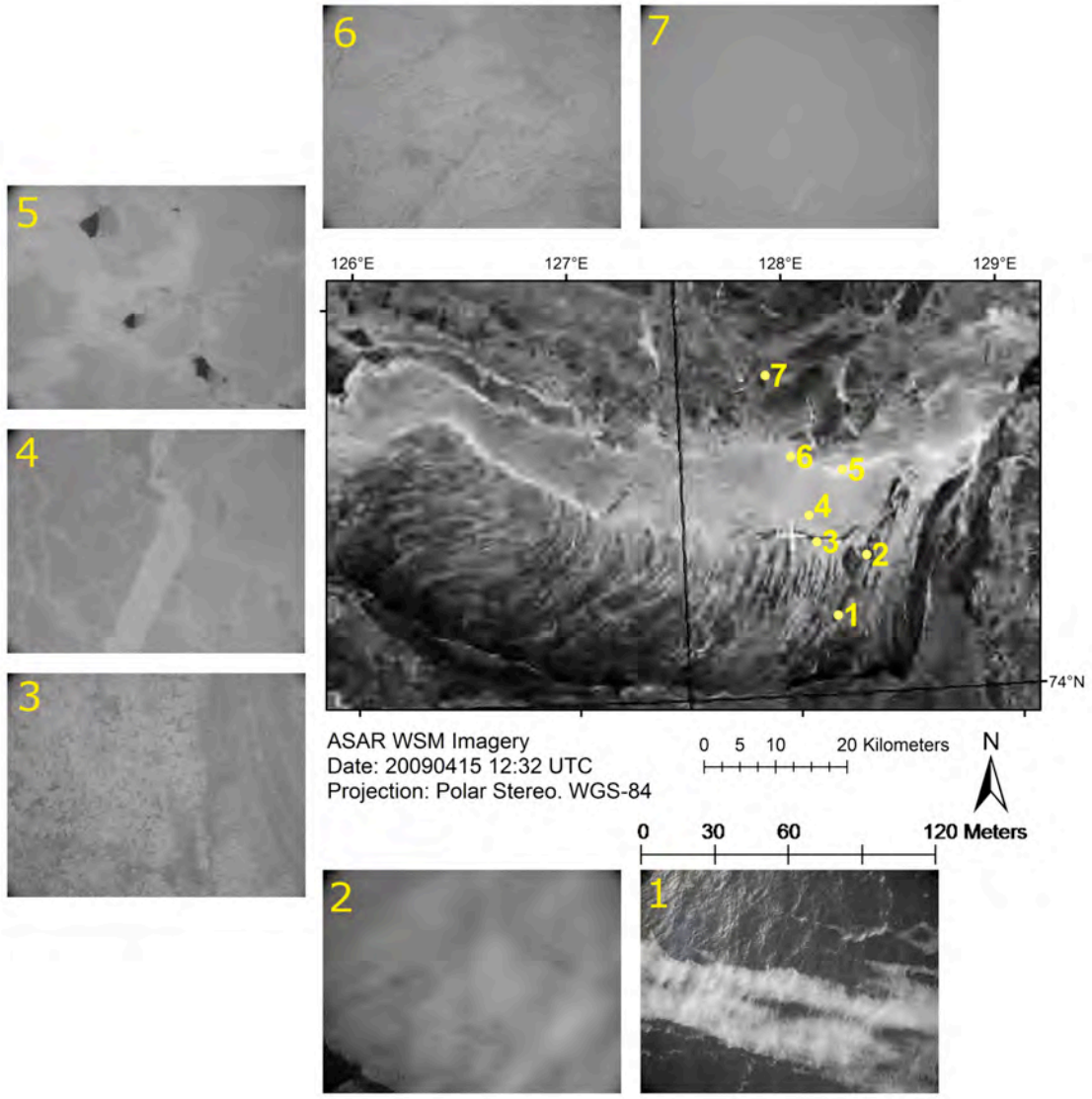

Fig. 6: ASAR image of the polynya event on April 15, 2009 and aerial photographs for selected positions (numbers) showing the ice conditions across the polynya.

Surface temperatures were derived from AVHRR or MODIS thermal infrared channels following the split-window method of Key et al. (1997) (see Fig. 5). Surface temperatures, acquired in the absence of direct solar radiation, simplify the inversion to ice thickness. The TIT was calculated using the surface energy balance model suggested by Yu and Lindsay (2003) with the aid of NCEP or GME meteorological reanalysis data (Kanamitsu et al., 2002) (Fig. 7). The thickness retrieval is based on the assumption that the heat flux through the ice equals the atmospheric turbulent and longwave radiation fluxes. The method yields good results for ice thicknesses below 0.5 m assuming further that vertical temperature profiles within the ice are linear, the temperature at the bottom is known and no snow is present on top of the ice (i.e., Drucker et al., 2003).

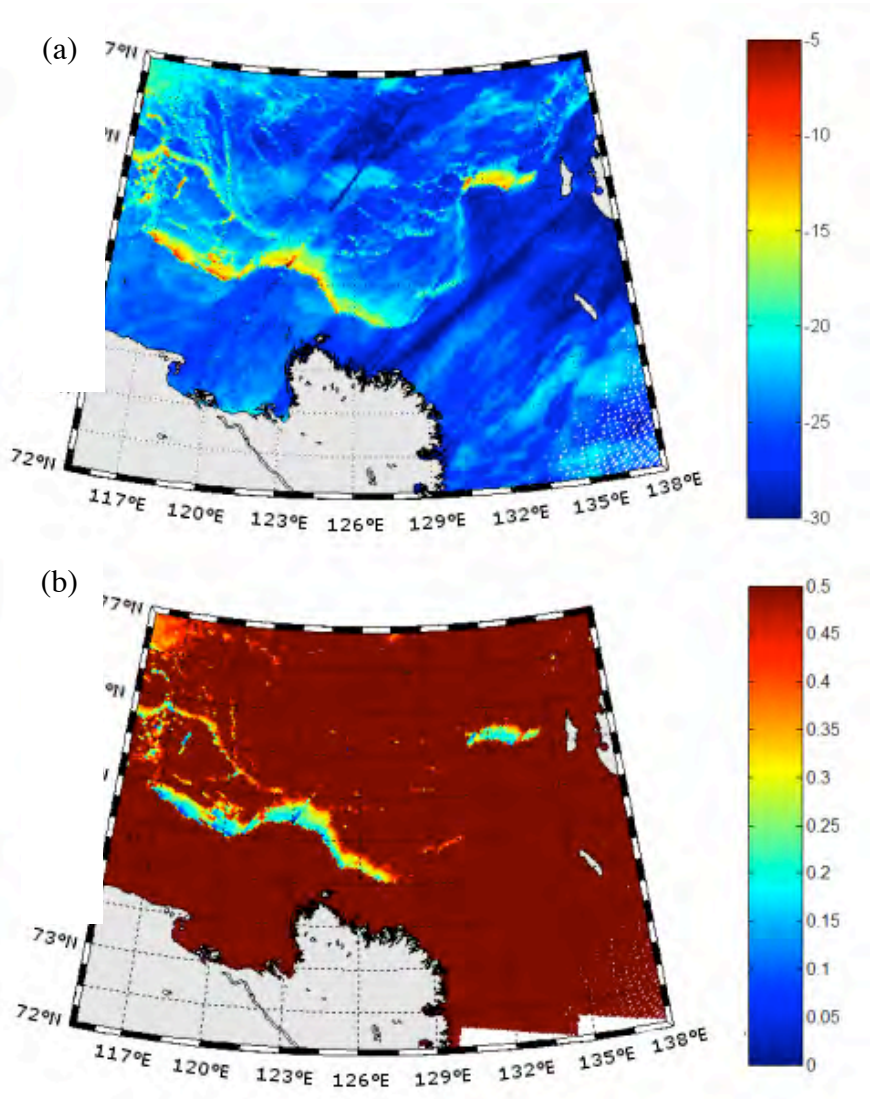

Fig. 7: (a) Surface temperature [°C] as derived from AVHRR IR brightness temperatures from March 27, 2009, 19:05 UTC. (b) Thermal ice thickness [m] as derived from the data in (a).

This method will be applied to the KT15 ice surface temperatures. Instead of reanalysis data we use the meteorological data measured during the expedition (see Chapter 2). We have to modify the algorithm because the KT15 ice surface temperatures are measured during daytime. Therefore, the short wave radiation must be included in the atmospheric fluxes. For calculation of the short wave radiation balance we use the measured meteorological data and determine the albedo of the different ice surfaces with the aid of the aerial photographs. The retrieved TIT will be validated with the measured reference profile.

1.4.2. Image geometry

All aerial pictures were taken with a GPS-compatible Ricoh© Capilo camera, mounted on a gimble. The external GPS antenna was placed outside the helicopter, approximately 2 m from the image centre point. The GPS position was taken every second. The used zoom focal length was 5.8 mm. The 35 mm equivalent is 28 mm with a view angle of 46.4° (β – vertical) x 65.5° (α – horizontal). After defining the image corner coordinates, photographs were georeferenced to a stereographic coordinate system using a cubic convolution methodology.

1.5. Profiles

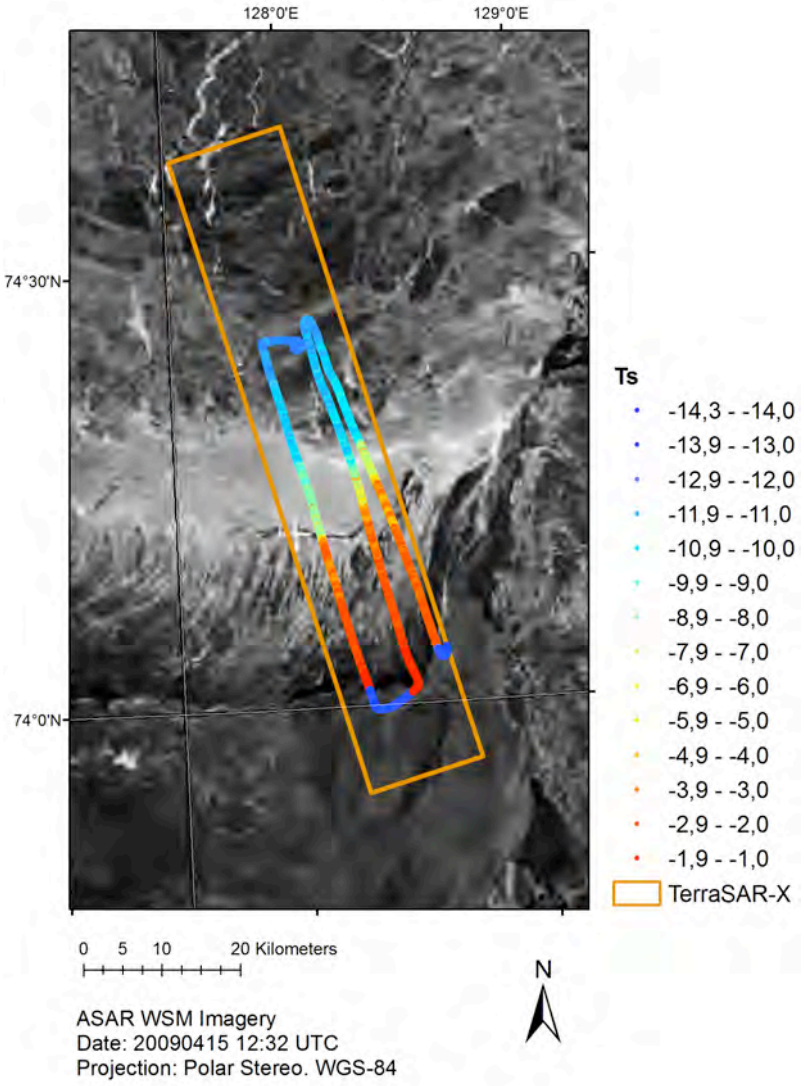

Fig. 8: Three remote sensing data sets from April 15, 2009. The orange frame denotes the TerraSAR-X frame, detected at 08:37 UTC. T_s is the ice surface temperature measured with the KT15 between 05:36 and 06:47 UTC. In the background the ENVISAT ASAR image detected at 12:32 UTC is shown.

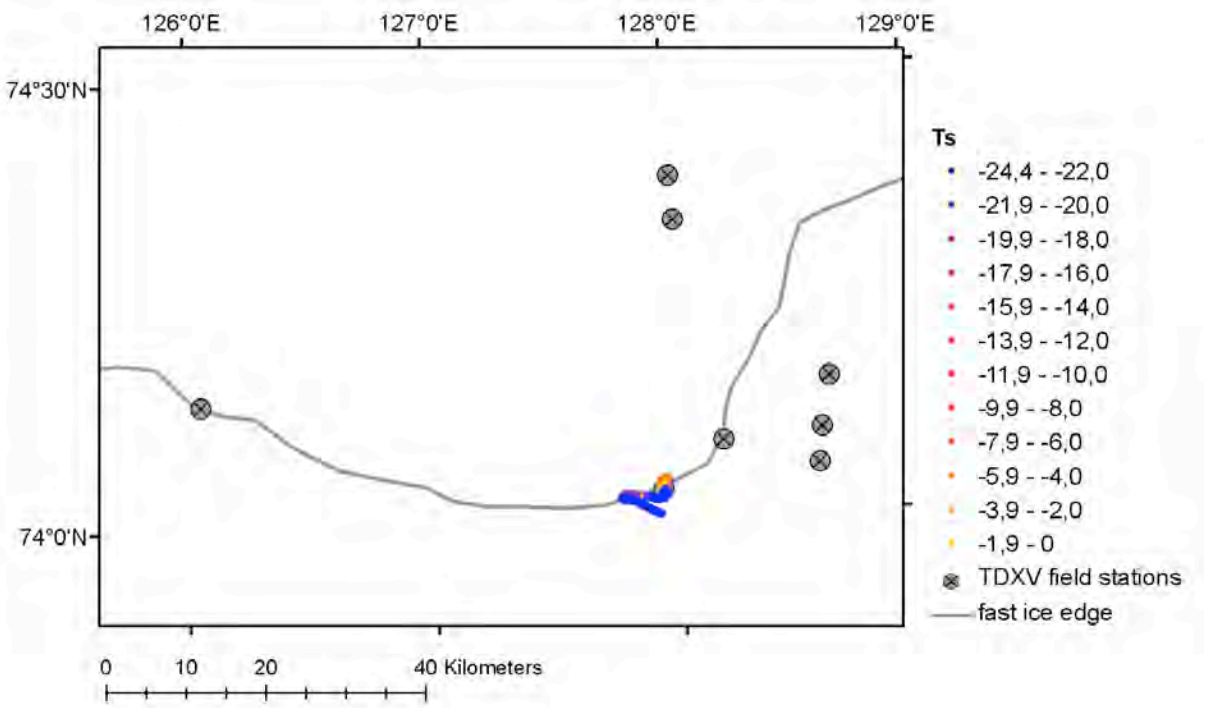

Fig. 9: KT15 profile on March 24, 2009 between 05:10 and 06:00 UTC (TI09-1).

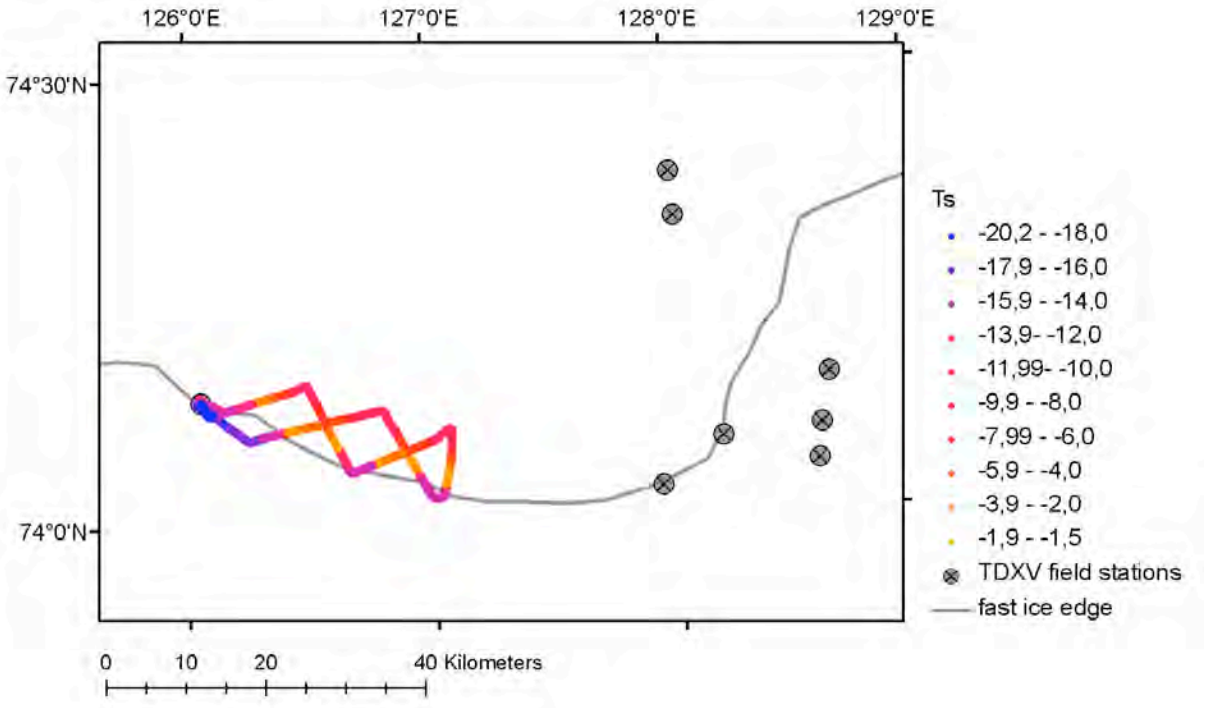

Fig. 10: KT15 profile on March 26, 2009 between 08:04 and 08:57 UTC (TI09-3).

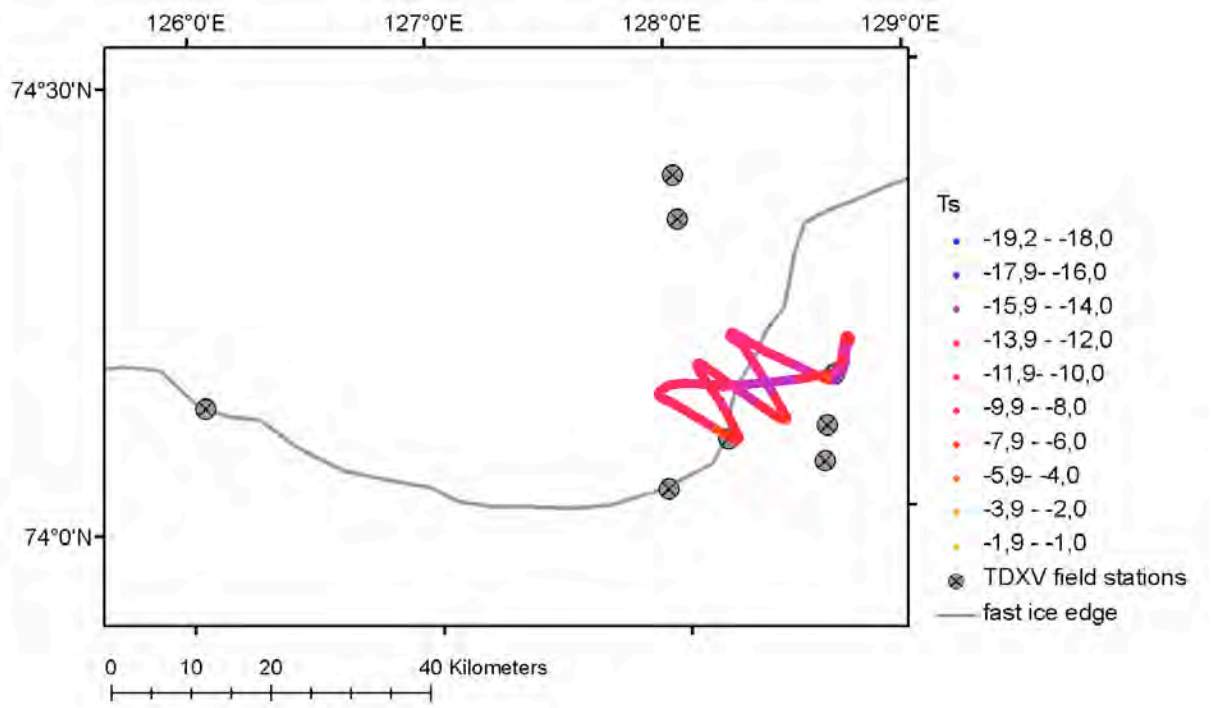

Fig. 11: KT15 profile on March 27, 2009 between 06:00 and 06:50 UTC (TI09-4).

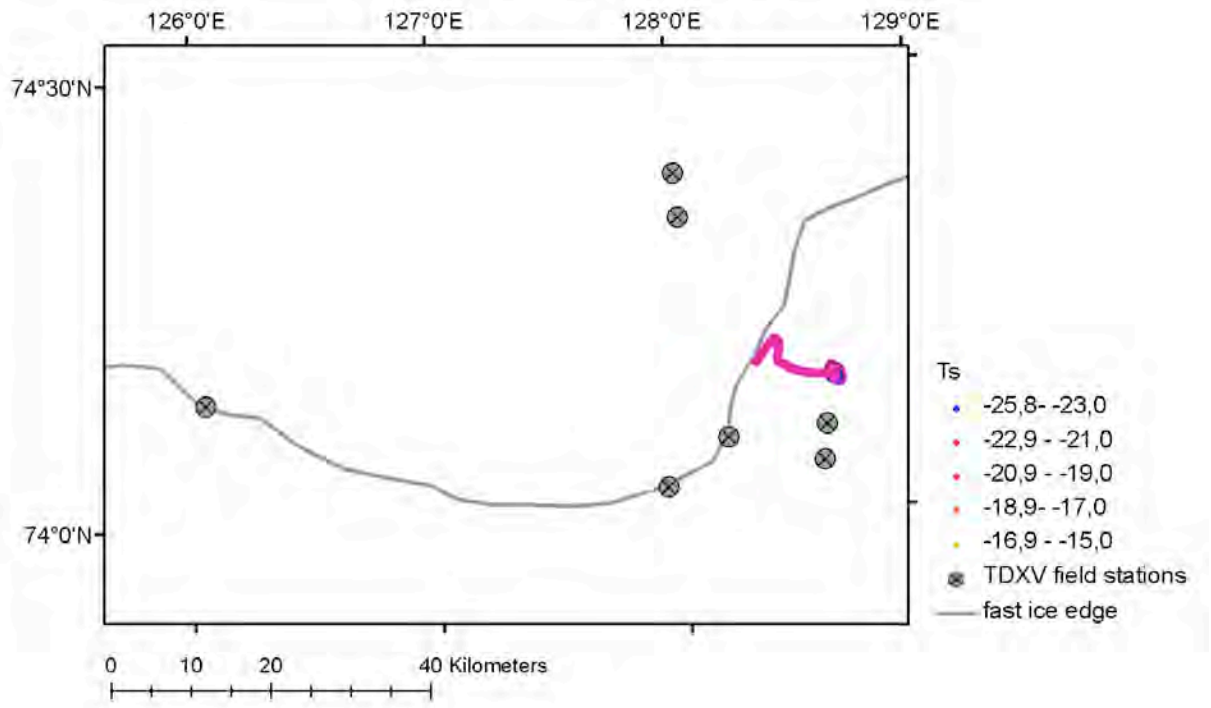

Fig. 12: KT15 profile on April 1, 2009 between 03:00-04:00 UTC (TI09-5).

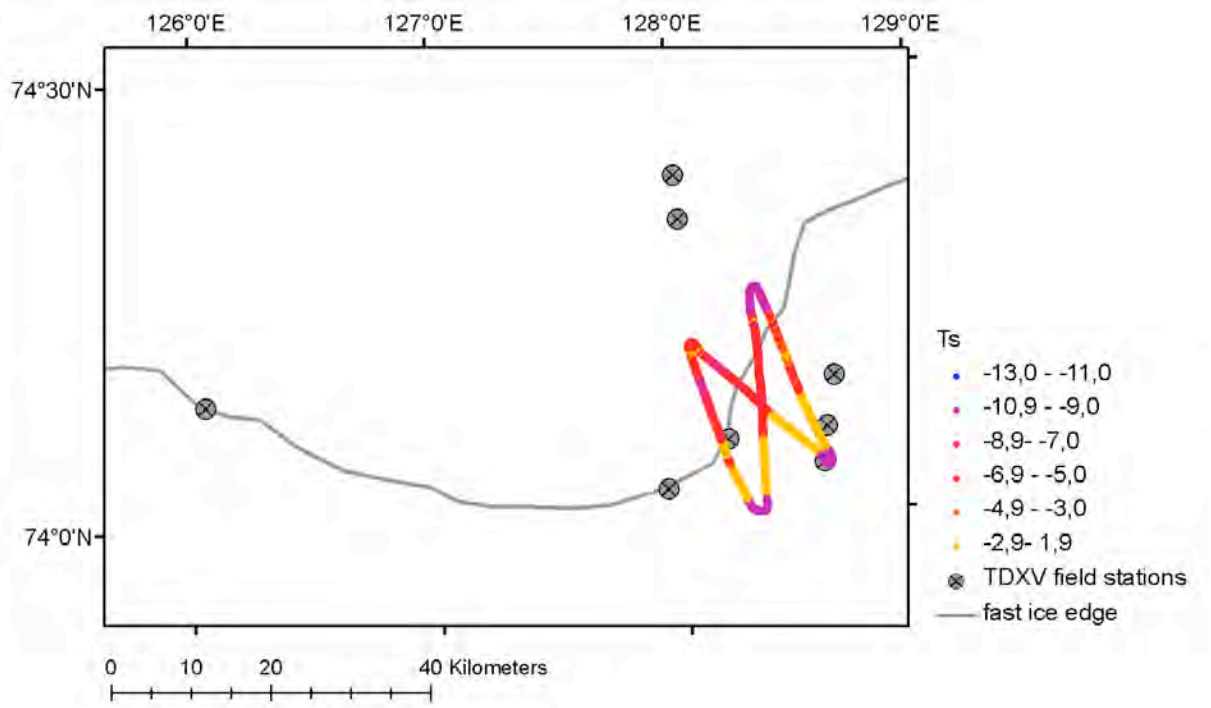

Fig. 13: KT15 profile on April 8, 2009 between 04:15 and 05:30 UTC (TI09-8).

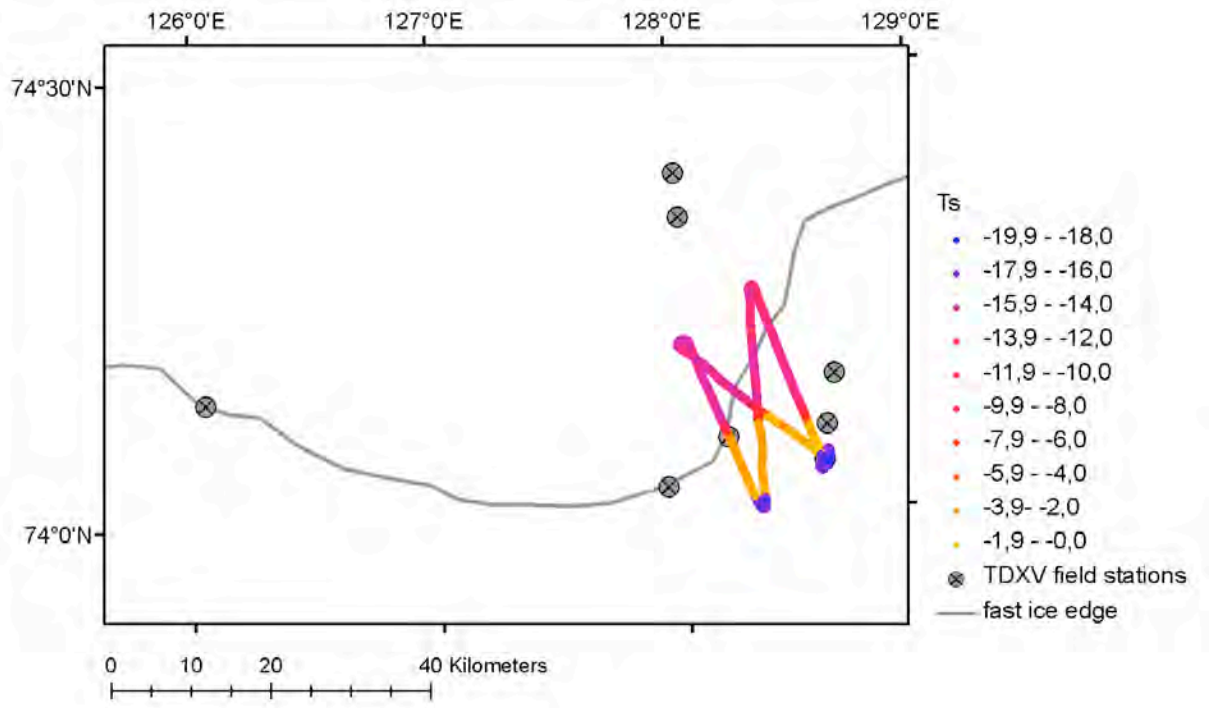

Fig. 14: KT15 profile on April 14, 2009 between 05:35 and 06:26 UTC (TI09-10).

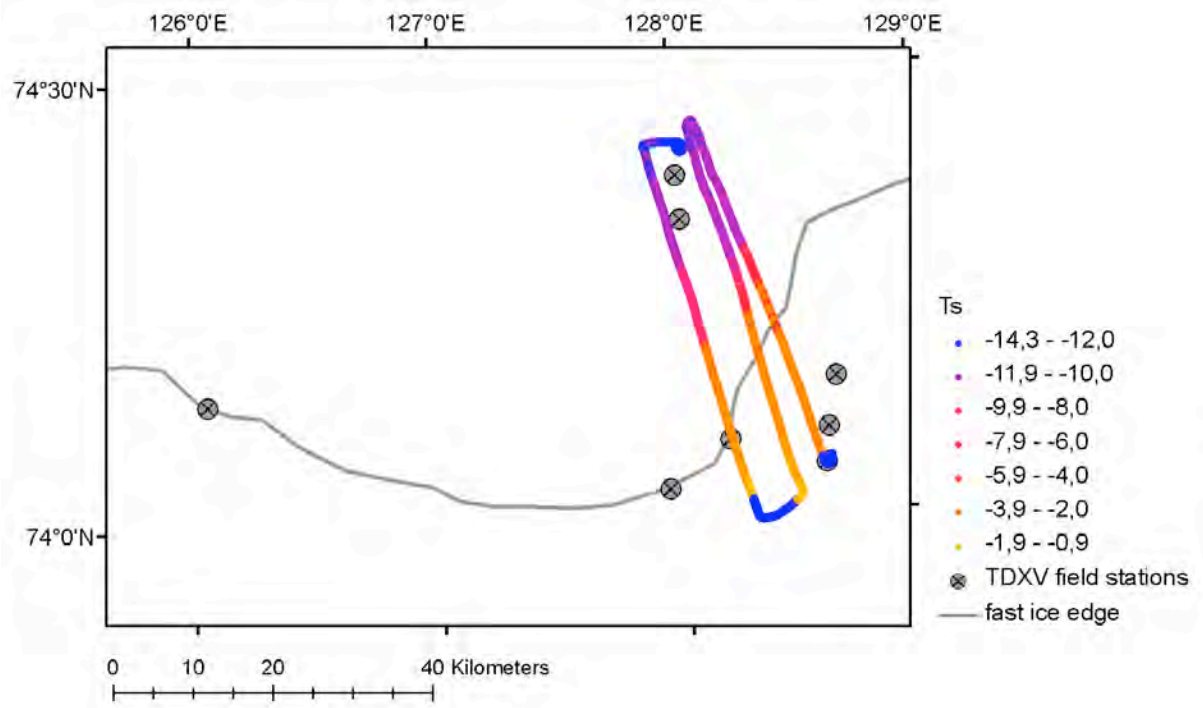

Fig. 15: KT15 profile on April 15, 2009 between 05:36 and 06:47 UTC (TI09-11).

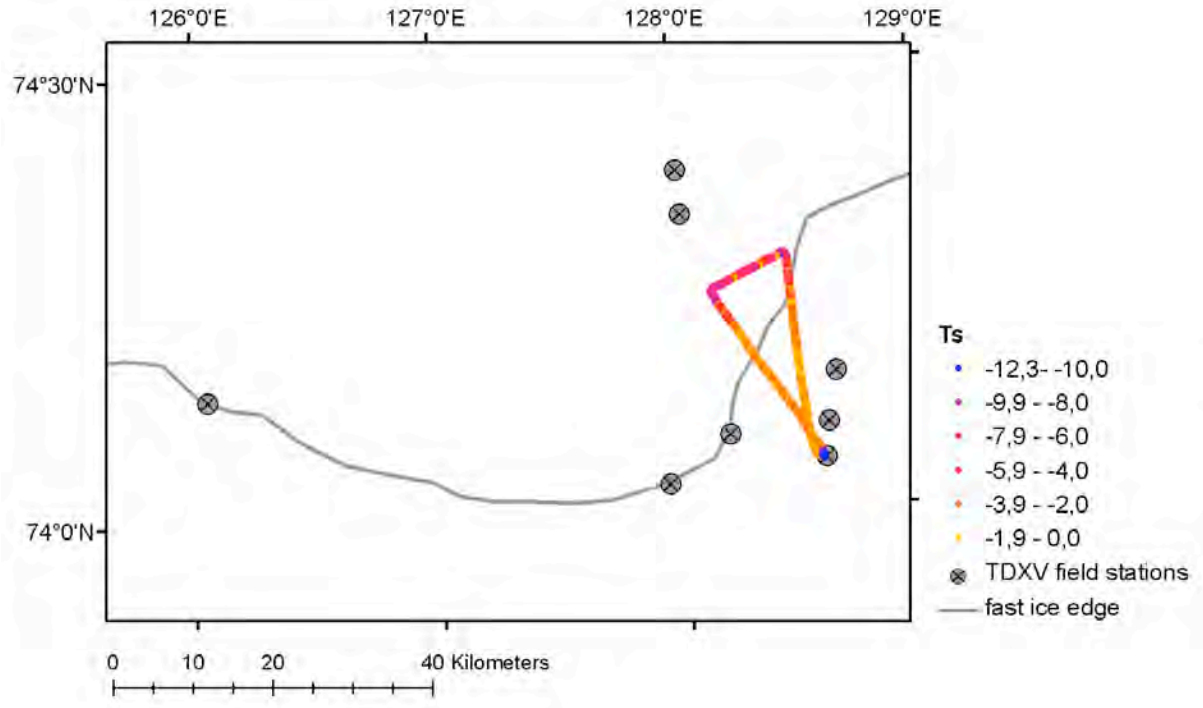

Fig. 16: KT15 profile on April 21, 2009 between 04:26 and 05:21 UTC (TI09-13).

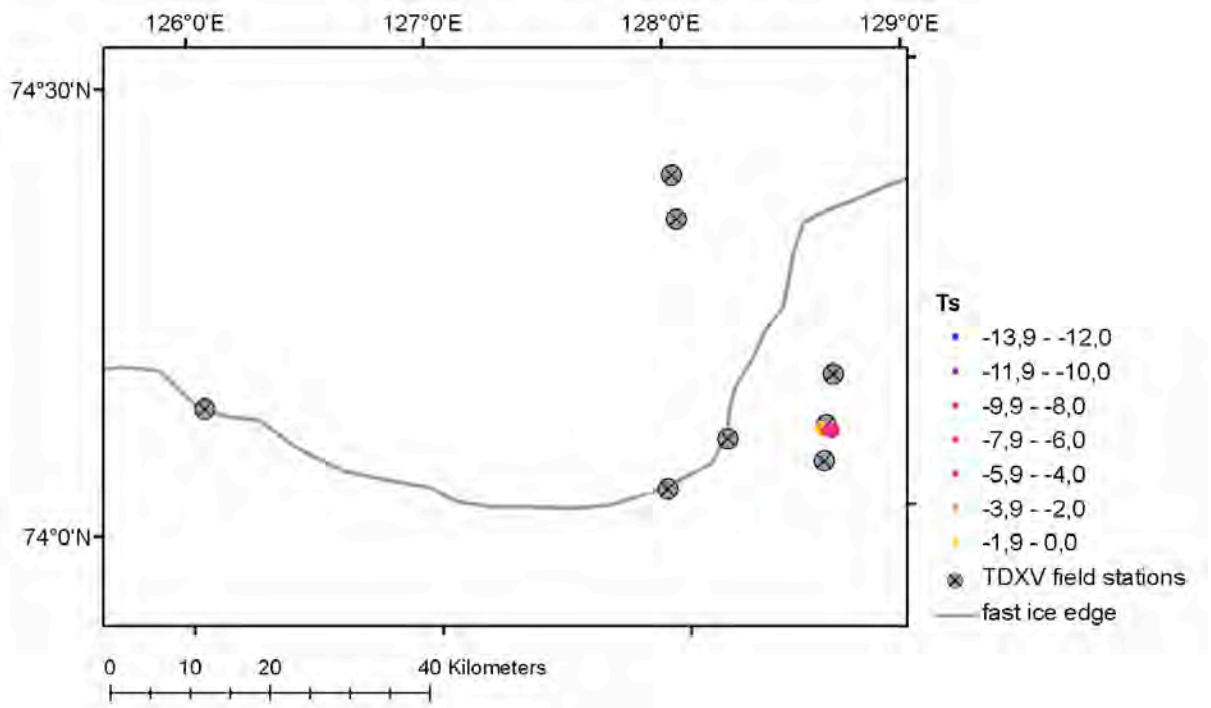

Fig. 17: KT15 profile on April 21, 2009 between 07:18 and 07:24 UTC (TI09-14).

2. Meteorological measurements at the ice edge of the west New Siberian Polynya

A. Helbig, S. Adams, G. Heinemann
University of Trier, Faculty of Geography / Geosciences, Dept. of Environmental Meteorology, Trier, Germany

2.1. Introduction

During the expedition TRANSDRIFT XV the meteorological regime was studied at four different sites along the ice edge of the West New Siberian Polynya during the period from March 24 to April 23, 2009 in high temporal resolution using Automatic Weather Stations (AWS).

This first data report provides information on the properties of the meteorological sensors, about the positions of the AWS and the volume of the collected data.

2.2. Description of AWS

2.2.1. Meteorological sensors

To ensure that the data loss was minimized, parallel measurements of air temperature and horizontal wind vector with different sensors on the AWS were carried out. The properties of the sensors are described below.

2.2.1.1. Wind speed and wind direction

- Ultrasonic Anemometer UsA 2D
  Range: 0-60 m/s, Accuracy +-2 %
  Resolution: 0.01 m/s
  Data rate: 1-4 Hz
  Output: Wind direction and wind speed or u and v-components
- Young Wind Monitor Model 05103
  Range: 0-100 m/s
  Resolution: Speed +-0.3 m/s, 1 %
  Direction: +-3°
  Starting speed: 1 m/s
  Signal: magnetically induced AC voltage, 3 pulses per revolution Azimuth potentiometer

2.2.1.2. Air temperature and humidity

- Campbell Scientific CS215; accuracy:
  Relative humidity: +-4%
  Air temperature: +-0.9 °C (-40°C to +70°C)
  The relative humidity sensor indicated refers to a saturation above water surface. The data set records contain the specific humidity (g/kg) instead of relative humidity.
- Electric ventilated thermometer (Typ Frankenberger)
  Platinum-Resistance Pt-100 according with DIN, tolerance +-0.1 K at 0°C

2.2.1.3. Net radiation

- NR_LITE Net Radiometer
  Thermopile (upper and lower sensors provide the differential temperature).
  Spectral range: 0.2-100 µm
  Directional Error (0-60° at 1,000 W/m^2):<30 W/m^2

Working temperature: -30°C to +70°C

The cooling of the thermopiles by the wind (wind speed U) decreases the temperature differemce between top and bottom used as the measure of the radiation balance Q_0. Therefore, Q_0 must be corrected using an empirical relationship specified by the manufacturer:

Q_0, cor = Q_0, obs U <=5 m/s

Q_0, cor = Q_0, obs * (1.0 + 0.021286 * (U – 5.0)) U >5 m/s

2.2.1.4. Surface temperature

- IR-Radiometer Apogee S-111, 22°
  Field of view: 22° half angle
  Wavelength range: 8-14 µm
  Accuracy (-40°C to 70°C): ±0.5 absolute accuracy

2.2.1.5. Barometric pressure

- Barometric Pressure Sensor RPT410F
  The barometric pressure readings in hPa were provided in relation to actual sensor height.

2.2.2. Height of sensors above ground

The AWS tripods were positioned directly on flat and smooth fast ice, and were vertically adjusted and fastened with ice screws. The sensors were mounted on each AWS at the same height above ground (fast ice). The snow cover on the fast ice varied between the four locations. The change of snow depth during the measurement period was negligible.

The sensor heights were as follows:

Air temperature, humidity: 2.0 m above snow
Net radiation: 1.6 m above snow
Wind speed, wind direction Young: 3.0 m above snow
UsA 2D: 2.8 m above snow
Surface Temperature: 0.4 m above snow

2.2.3. Data storage and transfer

For data storage a Data Logger Campbell CR1000 in conjunction with a memory card was used. The stored values are averages over 10 minutes and daily extreme values.

2.3. Sites of AWS

At all four sites identical AWS were deployed. The positions of the ice camps as well as the AWS are shown in Figure 18.

All times are related to UTC.

The local time is: Winter time to 28.3.09 Yakutsk Time YAT = UTC + 9 h
Summer time since 29.3.09Yakutsk Time YAT = UTC + 10 h

2.4. Positions of AWS

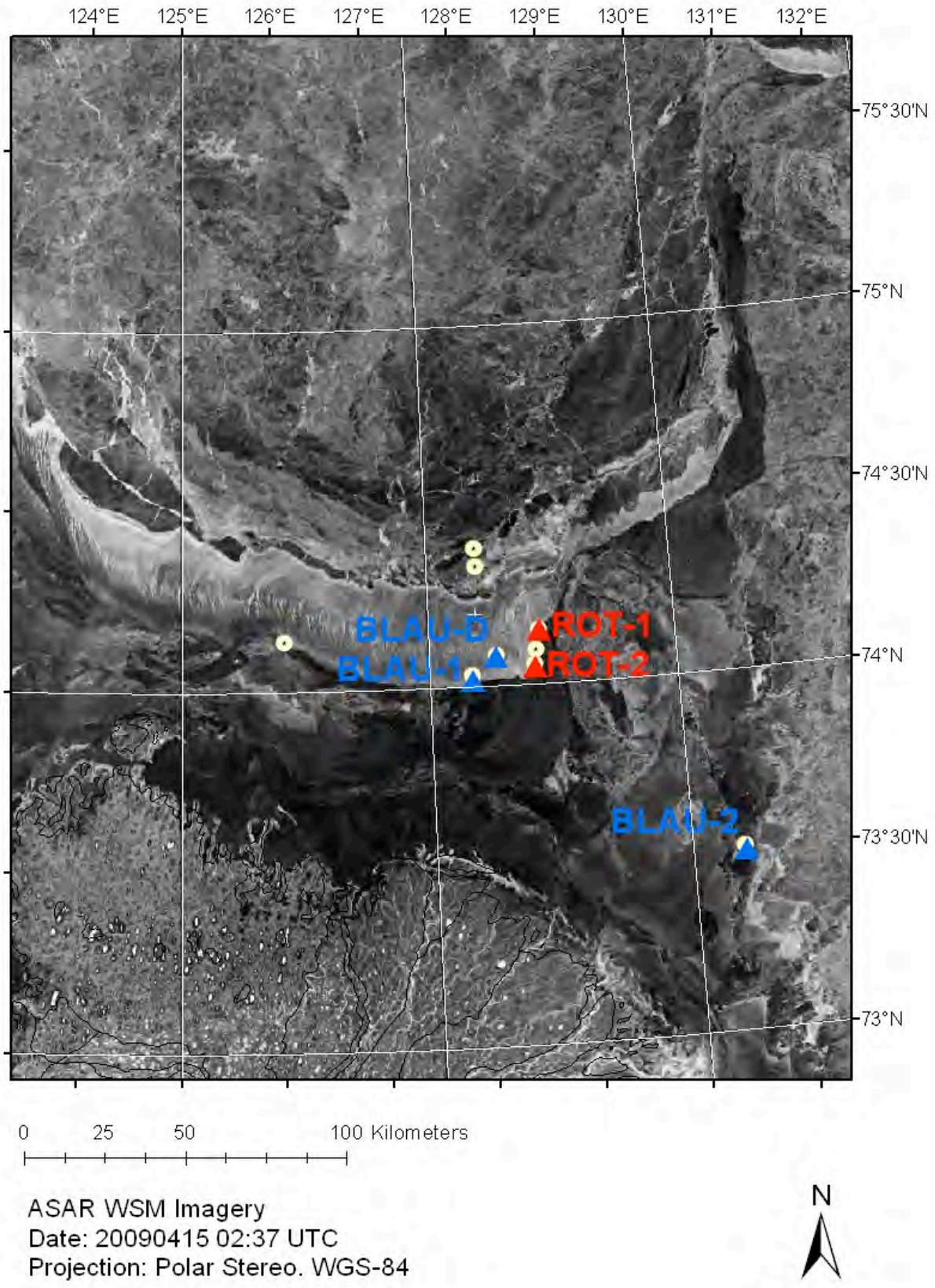

Fig. 18: Ice coverage and position of the West New Sibirian-Polynya on 15.4.2009 as well as the positions of stations. The AWS are located in the first phase at the stations BLAU-1/BLAU-D and ROT-1, in the second phase of observations at BLAU-2 and ROT-2.

2.4.1. Station POLYNYA-I/TI09-1

2.4.1.1. Installation

AWS ID: BLAU

Start of observations: 24.3.2009 5:00 UTC

Ventilation switched on; switched off if battery voltage lower than 11 V

Coordinates: 74° 01.981'N, 127° 56.212'E

Situation: Fast ice, depth 102 cm, snow cover ca. 5-7 cm, 150 m south of polynya ice edge, 100 m southeast of mooring station. Free air flow from all directions

Weather at the start of observations: Cloudless, visibility 10 km, wind SSE 4-6 m/s, air temperature -22.0°C, steam over the water surface

2.4.1.2. Changes

Inspection on 1.4.2009

An ice floe was broken from fast ice and drifted 9.72 km to NE with AWS to new location 1.4.2004, 6:01 UTCN, 74° 05.195'N, 128° 11.285'E

The AWS has considerable damages – all devices out of operation. Cables, plugs and sockets of the logger box are damaged.

All devices de-installed except the tripod.

2.4.1.3. De-installation

Inspection on 2.4.2009

Drift of ice floe was continued by 0.75 km to NE to the new location 2.4.2009, 1:56 UTCN, 74° 04.834'N, 128° 11.951'E

The tripod was de-installed.

2.4.2. Station POLYNYA-II/TI09-4

2.4.2.1. Installation

AWS ID: ROT

Start of observations 27.3.2009 6:05 UTC

Ventilation switched on; switched off if battery voltage lower than 11 V

Coordinates: 74° 09.039'N, 128° 38.132'E

Situation: Fast ice, depth 118 cm, snow cover ca. 5 cm, 150 m south of polynya ice edge, 80 m southwest of mooring station.

Free air flow from all directions. Smaller ice ridges in a distance of ca. 250 m. Newly formed ice is shifting from NW over the fast ice.

Weather at the start of observations: 8 Cs, visibility 15 km, wind SW 2-4 m/s, air temperature -14.1°C

2.4.2.2. Changes

Inspection on 1.4.2009

The AWS has considerable damages. Cables, plugs and sockets of the logger box are partly damaged.

Continuation of the observations at 4:00 UTC with CS215 (air temperature, humidity) and

NR_Lite_Net Radiometer only.

Weather at the restart of observations: 8 Cs, visibility >10 km, wind NW 4-6 m/s, air temperature -22.4 °C

2.4.2.3. De-installation

Inspection on 3.4.2009

De-installation of the station POLYNYA-II because newly formed ice was moving over the polynya ice edge.

End of observation with CS215 and NR_Lite_Net Radiometer at 2:30 UTC.

De-installation of the AWS.

Weather at de-installation of AWS: 5 Ci, 4 Ac, visibility 10 km, wind NW 1-2 m/s, air temperature -19.6°C

2.4.3. Station POLYNYA-III/TI09- 8

2.4.3.1. Installation

AWS ID: ROT (after repair)

Start of observations: 8.4.2009 5:05 UTC

Ventilation: No ventilation because motor out of operation

Coordinates: 74° 03.313'N, 128° 34.679'E

Remarks: The logger box was rotated by 180° to better protect the cable. On top of the logger box now a self-made tin box contains all cables. Plugs and sockets were replaced by lustre terminals. To all metal parts and to the cables, diesel oil was applied.

Situation: Fast ice, depth 116 cm, snow cover ca. 8 cm, snowdrift up to 15 cm.

Free air flow from all directions. 150 m east of mooring station, 1 km southeast of polynya ice edge.

Weather at start of observations: 7 Ac, As, visibility 15 km, wind SE 4-6 m/s, air temperature -9.2°C

2.4.3.2. Changes

Inspection on 14.4.2009, 7:00 UTC

Data are collected from April 8 to 14, 2009. No missing values. AWS was without damages. To all metal parts and to all cables, diesel oil was applied.

Weather at data collecting: Cloudless, snow blowing, wind S 8-10 m/s, air temperature -19.0°C

2.4.3.3. De-installation

De-installation of the AWS on 23.4.2009. End of observations at 4:30 UTC. No damages at the AWS.

Weather at de-installation: 8 St, light snow fall, wind SSE 4-6 m/s, visibility 3 km, air temperature -15.0°C

2.4.4. Station FAST ICE/TI09-9

2.4.4.1. Installation

AWS ID: BLAU (after repair)

Start of observations: 14.4.2009 4:00 UTC

Observations without electrical psychrometer

Coordinates: 73° 30.697'N, 130° 31.447'E

Remarks: The logger box was rotated by 180° to better protect the cable. On top of the logger box now a self-made tin box contains all cables. Plugs and sockets were replaced by lustre terminals. To all metal parts and to the cables, diesel oil was applied.

Situation: Fast ice, depth 170 cm, snow cover ca. 4 cm

Free air flow from all directions

Distance to POLYNYA-III: 86 km

Weather at start of observations: Cloudless, snow blowing, wind S 8-10 m/s, air temperature -18.6 °C

2.4.4.2. Changes

No changes

2.4.4.3. De-installation

De-installation of the AWS on 23.4.2009. End of observations at 6:45 UTC. No damages to the AWS.

Weather at de-installation: 8 St, light snow fall, wind SSE 5-7 m/s, visibility 2 km, air temperature -13.4 °C

2.5. Data structure

The periods of available data from the AWS at different sites are shown in Tables 3 and 4.

Table 3: Available data sets from AWS POLYNYA-I and POLYNYA-II

Position	March								April		
	24.	25.	26.	27.	28.	29.	30.	31.	1.	2.	3.
Polynya-I	■	■	■	■	▒	▒	▒	▒	▒		
Polynya-II				■	■	■	■	■	■	■	■

AWS at position: ▒

Data available (at least 3 parameters): ■

The observations by the AWS are provided in each four files (ASCII format)

Table 4: Available data sets from AWS POLYNYA-III and FAST ICE

Position	April															
	8.	9.	10.	11.	12.	13.	14.	15.	16.	17.	18.	19.	20.	21.	22.	23.
Polynya-III	■	■	■	■	■	■	■	■	■	■	■	■	■	■	■	■
Fast Ice							■	■	■	■	■	■	■	■	■	■

Data available (at least 3 parameters): ■

The observations by the AWS are provided in each four files (ASCII format)

3. Oceanographic investigations

S. Kirillov[1], I. Dmitrenko[2], T. Klagge[2], J. Hoelemann[3], M. Makhotin[1]
[1]Arctic and Antarctic Research Institute, St. Petersburg, Russia
[2]Leibniz Institute of Marine Sciences IFM-GEOMAR, Kiel, Germany
[3]Alfred Wegener Institute for Polar and Marine Research, Bremerhaven, Germany

3.1. Goals and research tasks

The main goal of oceanographic research activities during the expedition was to investigate the influence of the open water areas (polynyas) on the thermohaline and dynamic regimes of the Laptev Sea shelf waters during winter with special emphasis on the possible overcooling of the surface water layer in the polynya and beneath the fast ice cover produced by favorable meterological and ice conditions. In addition the oceanographical investigations were aimed at obtaining new data on the thermohaline state of the Laptev Sea waters during a single season, spatial and temporal distribution of oceanographic parameters in the polynya region, and seasonal variability of current velocities and directions on the Laptev Sea shelf. The research tasks were to:

- carry out repeated oceanographic measurements together with hydrochemical and biological sampling on the fast ice edge and drift ice;
- make 1-1.5 km long oceanographic profiles across the fast ice edge with 150 m intervals between observational sites;
- deploy 2 oceanographic bottom stations at the fast ice edge for the period of the expedition.

3.2. Oceanographic equipment

The following oceanographic equipment was used:

2 CTD probes SeaBird 19plus

The CTD probes were produced by Sea Bird Electronic (USA); one of the probes was equipped with additional sensors for dissolved oxygen, turbidity and chlorophyll. the main characteristics of the CTD probe are:

- operational depth: 7,000 m
- temperature measurement range: -2 to +40°C
- salinity measurement range: 0-40‰
- temperature measurement accuracy: ±0.005°C
- salinity measurement accuracy: ±0.001‰
- triggering time: 4 sec to18 hours
- vertical resolution from: 0.1 m

The CTD SBE 19plus probe allows measuring seawater temperature and salinity and hydrostatic pressure. The probe is additionally equipped with a dissolved oxygen sensor SBE 43 produced by Sea-Bird Electronics, Inc., USA, a chlorophyll *a* sensor produced by WetLabs, Inc. USA, and a turbidity sensor produced by Seapoint Sensors, Inc. USA. The accuracy of dissolved oxygen concentration measurement is -2% of saturation value and sensor stability is 2% for 1,000 hours. Chlorophyll *a* is measured at wave-lengths of 460 and 695 nm, sensitivity of the sensor is ≥3 µg/l. Turbidity is measured at wave-length of 880 nm.

4 probes SeaBird 37 Sea Bird Electronic (USA) with temperature and electrical conductivity sensors

The main characteristics are:

- operational depth: 7,000 m
- temperature measurement range: -5 to +35°C
- temperature measurement accuracy: 0.002°C
- electrical conductivity measurement range: 0.001-7.0 Sm/m
- electrical conductivity measurement accuracy: 0.0003 Sm/m

2 acoustic current meters ADCP Workhorse Sentiel 300 kHz

The main characteristics are:

- operational depth: 200 m
- velocity measurement range: -5 to +5 m/sec
- velocity measurement accuracy: 0.5% + 0.5 cm/sec
- current direction measurement accuracy: ± 2°

ADCP WH-S 300 kHz produced by Teledyne RD Instrument, USA was a component of bottom stations. It is designed to measure three components of current velocity and the intensity of backscatter signal.

Sub-ice bottom stations

During the expedition 2 sub-ice bottom stations were deployed. The complete set of such a station is shown in Figure 19. However, because of active ice-ridging one of the stations (TD09-01) was recovered and re-deployed in another position (TI09-08) and then successfully recovered while the second station (KD09-04) was lost. The list of equipment installed on the sub-ice bottom stations TD09-01 and TD09-08 and measurement characteristics are given in Table 5.

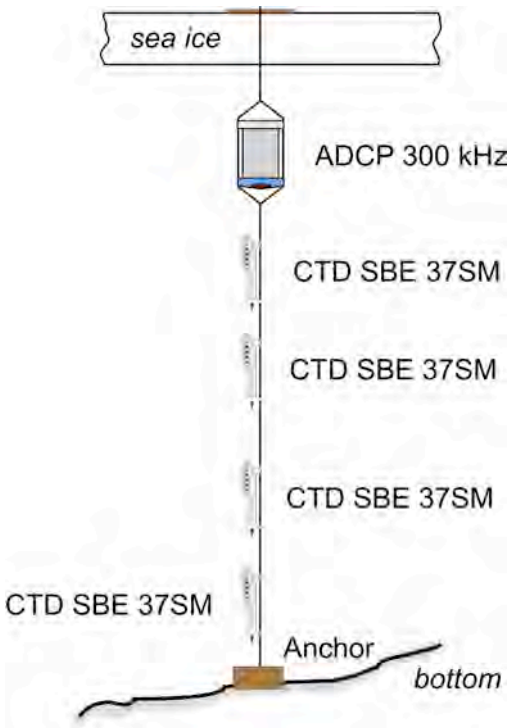

Fig. 19: General scheme of the deployed sub-ice bottom stations.

Table 5: Characteristics of the measuring devices of the sub-ice bottom stations

Site	Coordinates	Device	Fixation depth	Operational time period	Measuring interval
M09-1	74° 2.0'N 127° 56.1'E	ADCP current meter	~2.5 m	05:00, March 24, 2009 - 02:00, April 2, 2009	5 minutes
		CTD-probe SBE37	~2 m	09:00, March 24, 2009 - 2:22, April 2, 2009	1 min
		CTD-probe SBE37	~9 m	— // —	1 min
		CTD-probe SBE37	~16 m	— // —	1 min
		CTD-probe SBE37	~25 m	— // —	1 min
M09-2	74° 3.3'N 128° 34.5'E	ADCP current meter	~2.5 m	05:00, April 8, 2009 - 04:00, April 23, 2009	5 minutes
		CTD-probe SBE37	~2 m	08:00, April 8, 2009 - 4:13, April 23, 2009	1 min
		CTD-probe SBE37	~8 m	— // —	1 min
		CTD-probe SBE37	~15 m	— // —	1 min
		CTD-probe SBE37	~23 m	— // —	1 min

3.3. Methods

Vertical CTD measurements were carried out from fast or drift ice in close vicinity of the polynya. The holes in the ice were drilled with a motor drill. In order to reduce the error of measurements, caused by ice crushing during drilling, and sensor cooling under low air temperatures, the CTD probe was kept under ice for some time, and the measurements were taken repeatedly.

CTD measurements were carried out before the deployment of the sub-ice bottom stations in order to determine the water depths at the sites and to select the depths for fixing the instruments. The latter were dependent on the main or seasonal pycnocline position and the presence of a warm intermediate water layer or bottom layer of warm water advected with reversed currents. Later, the load and the rope with the fixed instruments were slipped down a special hole of a bigger diameter. The upper end of the rope was fixed on the ice surface. The station recovery was made with the help of a special tripod fixed above the hole.

3.4. Activities

In total, 29 CTD measurements were carried out at 15 oceanographic stations (Table 6; Fig. 1 in the chapter "Introduction"). At some sites the oceanographic measurements were repeated several times. This gave an idea about the transformations of the vertical thermohaline structure. For instance, at the site of station TI09-08 five oceanographic stations were carried out during 2 weeks, on April 8, 14, 15, 21 and 23. Two sub-ice bottom stations were deployed and recovered at the sites of the oceanographic stations TI09-01 and TI09-08 (M09-1 and M09-2, respectively).

The ADCP Sentiel 300 kHz measures the profile of 3 components of current velocity and the intensity of the backscatter signal in the overlying water layer. The CTD probe SBE-37 measures temperature, salinity and pressure at the fixed point at a certain depth.

Table 6: Oceanographic stations of the TRANSDRIFT XV expedition

#	date	Longitude, °E	Latitude, °N	#	date	Longitude, °E	Latitude, °N
TI09-01	24.03.09	127.935	74.033	TI09-09	14.04.09	130.526	73.512
TI09-02	26.03.09	128.027	74.334	TI09-10	14.04.09	128.565	74.058
TI09-03	26.03.09	126.057	74.141	TI09-11	15.04.09	128.020	74.381
TI09-04	27.03.09	128.634	74.151	TI09-12	15.04.09	128.565	74.058
TI09-05	01.04.09	128.634	74.151	TI09-13	21.04.09	128.564	74.058
TI09-06	02.04.09	128.197	74.081	TI09-15	23.04.09	128.566	74.058
TI09-07	03.04.09	128.635	74.151	TI09-16	23.04.09	130.522	73.513
TI09-08	08.04.09	128.575	74.055				

3.5. Preliminary scientific results

The CTD measurements revealed the main characteristics of the vertical thermohaline water structure in the central Laptev Sea region adjacent to the polynya. This year the surface water layer was strongly freshened. Its salinity was 5-8 psu lower that the average winter values in this region. In spring 2008 the measured surface water salinity was close to the climatic average values for this period (Fig. 20). Taking into account the absence of any other freshwater sources during this period, it might be concluded that the Lena River runoff water spread beneath the fast ice cover. The thickness of the freshened surface layer was only 2-3 meters (Fig. 21).

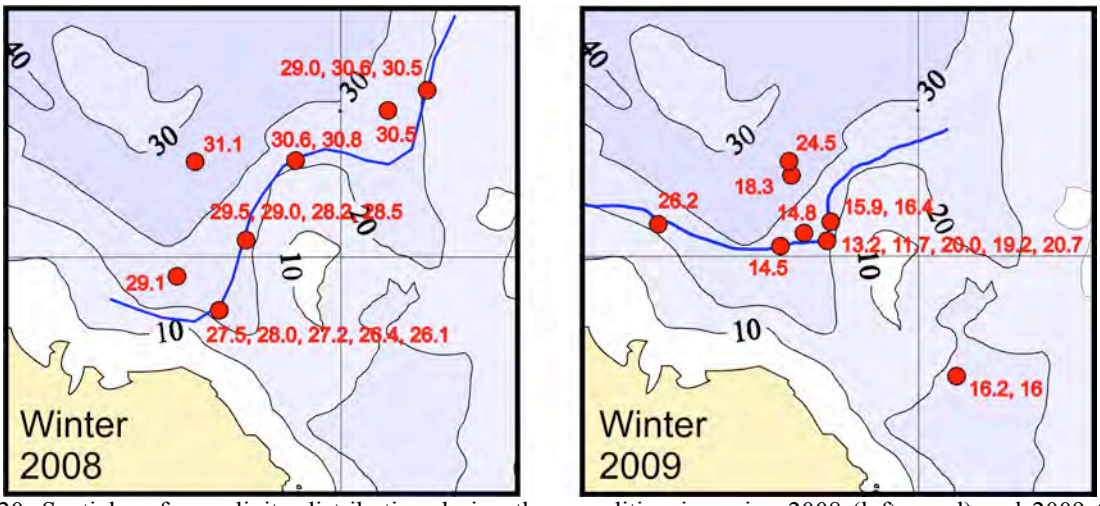

Fig. 20: Spatial surface salinity distribution during the expedition in spring 2008 (left panel) and 2009 (right panel). Salinity values are given in accordance with station numbers in Figure 2 in the chapter "Introduction." The blue line shows the fast ice edge position.

On the whole, the local vertical stratification is typical for this time of the year. The upper water column is occupied by a 5-15 m thick freshened mixed layer with a salinity ranging from 11 to 26 psu and a temperature close to freezing point. This layer is formed in the central Laptev Sea as a result of the offshore spreading of the Lena River runoff plume, wind and wave-induced mixing, and winter convection induced by sea ice formation and brine release. The bottom water layer is characterized by more saline and cold waters separated from the upper mixed layer by a strong pycnocline (Fig. 21, 22). The strong density change is largely due to the vertical salinity gradient since water temperature is close to the water temperature of maximum density and its influence is negligible.

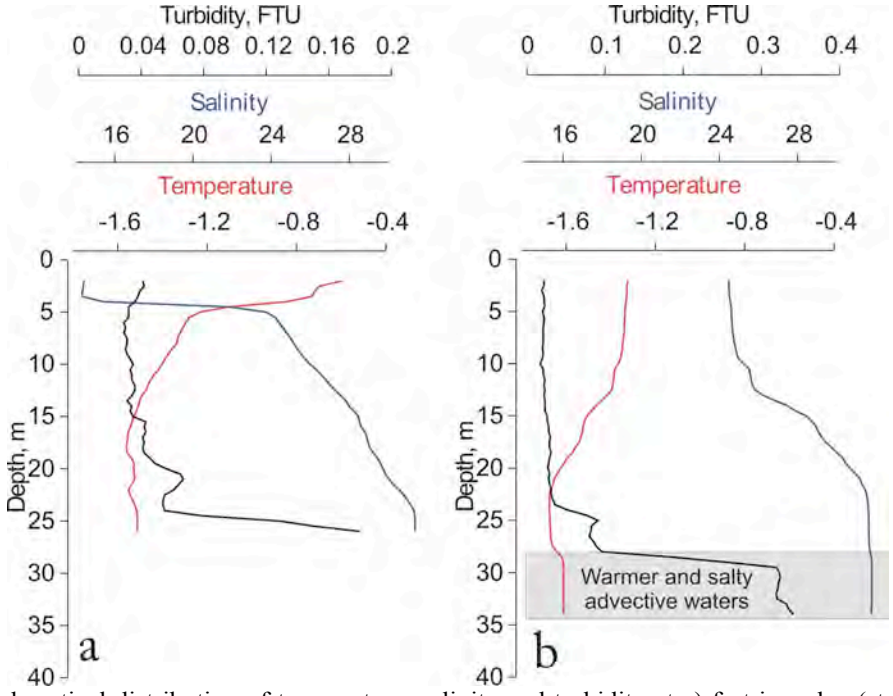

Fig. 21: Typical vertical distribution of temperature, salinity and turbidity at a) fast ice edge (station TD09-01) and b) drift ice in the polynya (station TD09-11).

The processes of sea ice formation in the polynya produce a specific pattern of the spatial salinity distribution in the surface water layer. Whereas under the fast ice (stations TI09-09 and TI09-16) and at the fast ice edge (stations TI09-01, TI09-04, TI09 06-08, TI09-10) the density gradient is well expressed, in the central part of the polynya under the drift ice (stations TI09-02, TI09-03 and TI09-11) and also at three stations at the fast ice edge (stations TI09-12, TI09-13 and TI09-15) the pycnocline layer is much less evident down from the 5 m level (Fig. 21, 22). At the three last stations, which were located at the position of the earlier stations TI09-08 and TI09-10, the observed difference in the vertical structure at the beginning and at the end of the expedition was most likely a result of enhanced vertical mixing due to the opening of the polynya under prevailing southerly winds. A considerable opening of the polynya (polynya event) was recorded by the instruments between April 15 and 23. During this period an open water area with new ice occurred 8-10 km off the fast ice edge, and the freshened surface water layer completely mixed with the underlying layers.

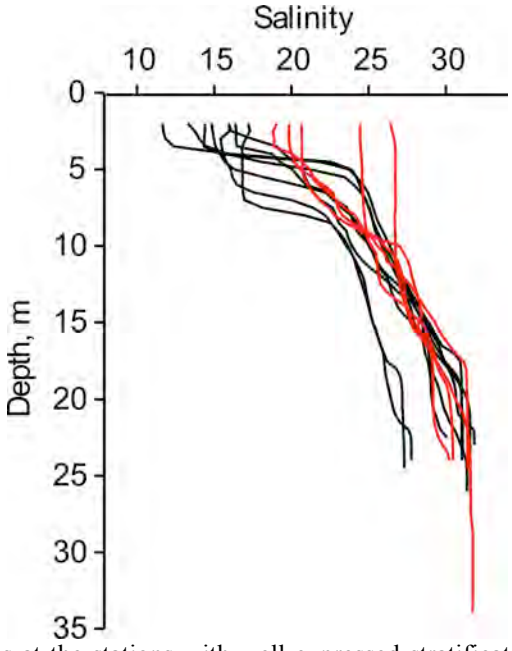

Fig. 22: Vertical salinity profiles at the stations with well expressed stratification and pycnocline (black lines) and at the stations with stratification disturbed by polynya processes (red profiles).

This explanation is supported by the analysis of temperature variability recorded at the site of bottom station M09-2 (Fig. 23). A strengthening of southerly winds resulted in enhanced wind-induced mixing in the open-water region located northwestward from this site. Due to the reversal character of tidal currents it was possible to record these changes of the vertical water structure in the open-water region because the water was advected from the open water beneath the fast ice cover for a distance of several kilometers.

Unfortunately, due to unknown reasons, we failed to obtain reliable electrical conductivity records from stations M09-1 and M09-2, which could have be used for salinity calculations. Therefore, it is impossible to estimate the overcooling of the surface water layer. Most likely, the electrical conductivity sensors failed because they were overcooled during the time when the station was prepared for deployment and then got ice-covered when put into the water.

Tidal currents are one of the factors determining the dynamics of the sub-ice water layer and the formation of the thermohaline regime in the region close to the polynya boundary. The data on current velocity distribution in the water column recorded by the current profiler allowed us to calculate the tidal components of the currents and their vertical variability. The main attention was paid to two harmonics, lunar (M2) and solar (S2) semidiurnal, which are major contributors to the energy of tidal movements in the region under study. The vertical distributions of both components of tidal current velocity show the same pattern whereas the amplitudes are different. In the report we present the results of the calculations of the lunar semidiurnal harmonic M2, which has a higher amplitude than S2.

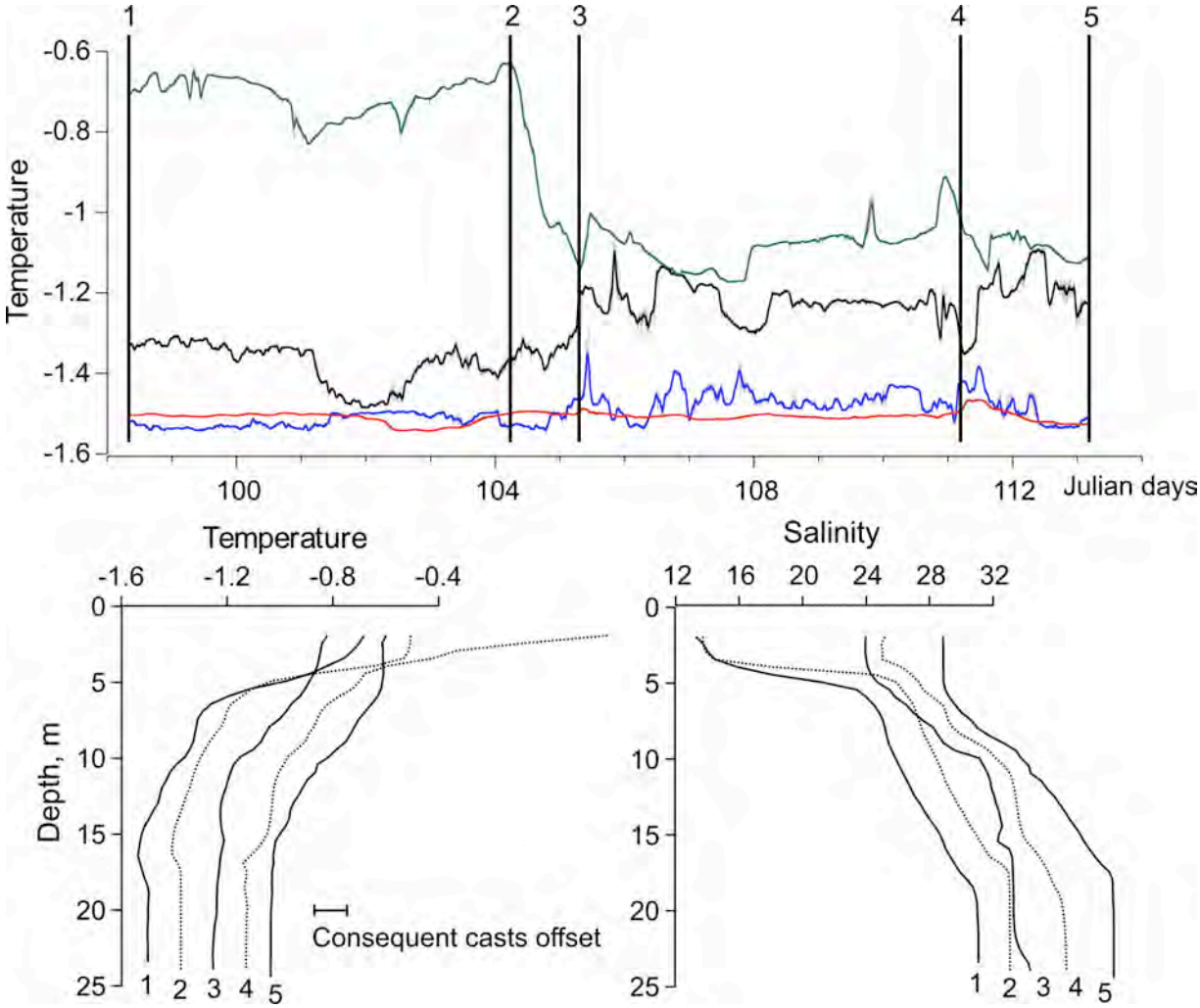

Fig. 23: Temperature time series (upper panel) at the depths of 23 m (red line), 15 m (blue line), 8 m (black line) and 2 m (green line) recorded by oceanographic bottom station TD09-08 during April 8-23, 2009. Lower panel shows vertical temperature and salinity profiles obtained at the same site during repeated measurements at episodic oceanographic stations (1: TD09-08, 2: TD09-10, 3: TD09-12, 4: TD09-13, 5: TD09-15). Temperature and salinity scales are linked to the first profile.

A comparative analysis of the data obtained in April 2008 and 2009 revealed a similar vertical distribution of velocities on the frequency of the lunar semidiurnal component of tidal currents at the stations located at the fast ice edge (Fig. 24). The velocity values increase with depth and reach their maximum at 15-16 m. Further down they decrease to minimum values in the bottom water layer (Fig. 24). On the whole, tidal current velocity was higher in 2008 than in 2009. The maximum value of the M2 component of 95 mm/s was recorded at the depth of 15 m in 2008. The maximum value in the surface water layer at the depth of 7 m was also recorded in 2008 and reached 65 mm/s whereas in 2009 it was 16 mm/s. This difference might be attributed to the interannual variability of the spatial fast ice edge configuration, which strongly affects the spreading and transformation of the tidal wave in the shallow shelf region.

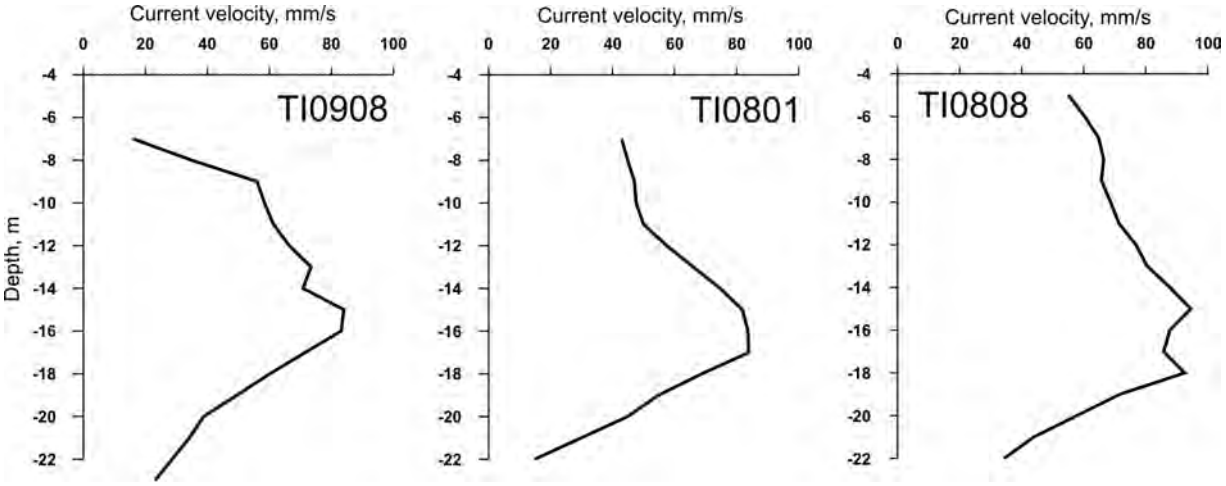

Fig. 24: Vertical profiles of the value of the main axis of tidal current ellipse on the frequency of lunar semidiurnal harmonic M2 calculated for April 2008 and 2009. Observational data from stations TI09-08, TI08-01 and TI08-08 with coordinates 74.06 N 128.58 E located on the fast ice edge.

For 2008, also the tidal current ellipses of the M2 component were calculated for the stations located southwest (TI08-02) and northeast (TI08-04) of the site of oceanographic bottom station M09-2 (Fig. 25). The calculation results show a similar enhancement of the tidal wave in the intermediate layer. However, absolute current values at station TI08-02 are much higher than those calculated for station TI08-04. The maximum value for station TI08-02 was 156 mm/s at 11 m water depth whereas the same value for station TI08-04 was only 61 mm/s at the depth of 14 m.

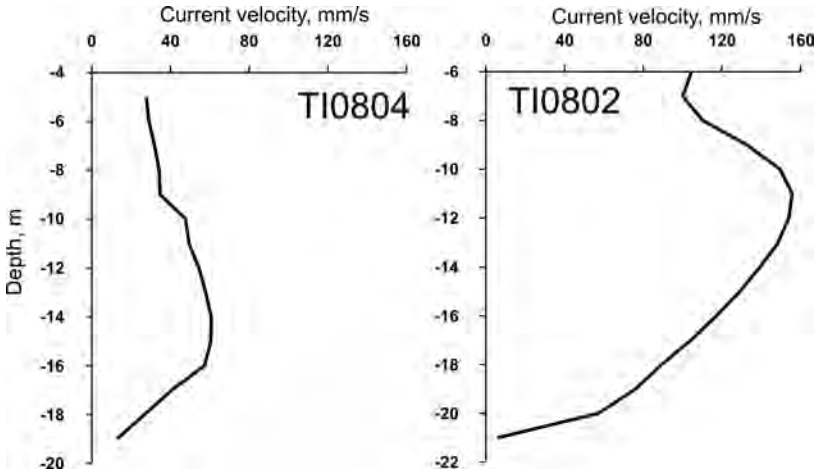

Fig. 25: Vertical profiles of the value of the main axis of the tidal current ellipse on the frequency of lunar semidiurnal harmonic M2 calculated for April 2008. Observational data from stations TI08-04 with coordinates 74.39'N, 129.32'E and TI08-02 with coordinates 73.81'N, 128.16'E.

4. Hydrochemical investigations

J. Hoelemann[1], E. Bloshkina[2]
[1]Alfred Wegener Institute for Polar and Marine Research, Bremerhaven, Germany
[2]Arctic and Antarctic Research Institute, St. Petersburg, Russia

4.1. Introduction

The Laptev Sea is a high arctic shelf sea that is strongly influenced by river runoff in summer and severe sea-ice conditions during wintertime. Recent investigations revealed that summer and winter processes have a distinctly different influence on the redistribution of river runoff on the shelf, the density stratification of the water column, and the transport and pathways of organic and inorganic matter. The study of the hydrochemical parameters (macro-nutrients, dissolved oxygen) during different seasons of the year can help to obtain a better understanding of the temporal and spatial variability of the environmental processes in the Laptev Sea.

One of the most important processes affecting the ocean/atmosphere interactions in the Laptev Sea is the system of wind-induced flaw leads and polynyas which is formed in winter between the fast ice cover and drift ice. These areas of open water or young ice might be up to 100 km wide. Extremely low air and water temperatures result in active sea ice formation and brine release causing a local increase of salinity in the upper water column.

In order to reveal the features of the hydrochemical regime in connection with the occurrence of polynyas, chemical investigations during the TRANSDRIFT XV expedition focused on the following tasks:

- the investigation of the spatial and temporal distribution of hydrochemical characteristics in the polynya area;
- a study of the seasonal and multiannual variability in the distribution of hydrochemical parameters;
- an assessment of the influence of polynyas on the hydrochemical and biological cycles in a shallow Arctic shelf sea.

4.2. Sampling and Methods

Water was collected with 2-liter plastic water samplers (Niskin type) through 22 cm wide holes that were drilled through the ice. To protect the water samplers from freezing, the sampling took place in a heated tent. Samples for oxygen concentration were taken first from the samplers and filled into 100 ml glass bottles. Subsequent to the sampling the dissolved oxygen was precipitated by adding 1 ml of manganese chloride and 1 ml of potassium iodide/sodium hydroxide solution. The sample was then shaken until an evenly distributed precipitate formed. The dissolved oxygen content was determined by titration with sodium thiosulfate using an electronic burette ABU-80 following the modified Winkler method. In addition the dissolved oxygen content was measured *in situ* with an SBE-43 sensor installed on the oceanographic SBE19 plus probe.

Water samples for nutrients (nitrite, nitrate, phosphate, and silicate) were collected in 50 ml plastic bottles. Immediately after sampling the bottles were frozen to -20ºC (minimum) and later transported to the Russian-German Otto-Schmidt Laboratory for Polar and Marine Sciences in St. Petersburg (OSL) for further analysis. The concentrations of nutrients in seawater were measured with an automatic segmented flow analyzer SKALAR Sun Plus system.

The water samples for the gravimetric determination of the suspended matter concentration were filled into 500 ml plastic bottles and later filtered trough pre-balanced Millipore filters (HVLP) with a pore size of 0.45 µm. To remove sea salt, the filters were washed with distilled water and then dried.

4.3. Preliminary results

During the expedition water samples were taken at 13 oceanographic stations in the Laptev Sea (Fig. 26). The total number of samples and the number of processed samples are shown in Table 7. 18 oxygen samples could not be analyzed because the time period between sampling and analysis in the laboratory in Tiksi was too long to yield accurate results.

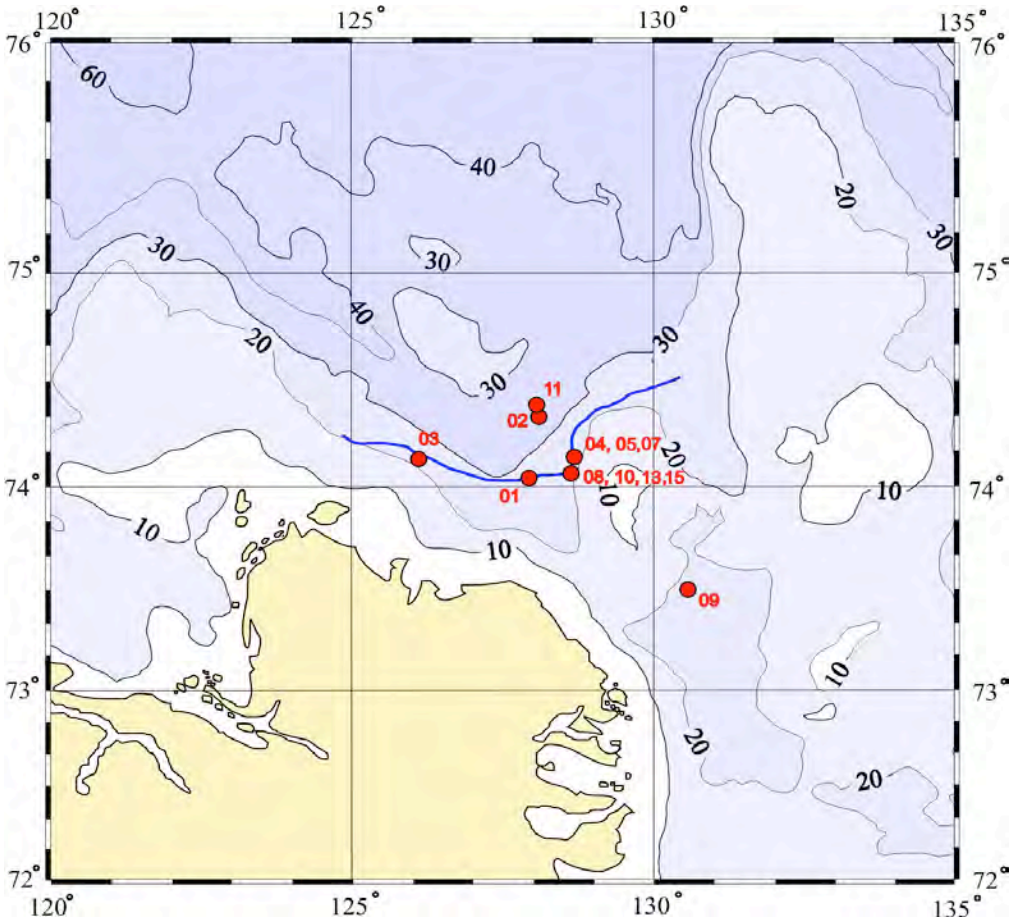

Fig. 26: Water sampling sites.

Table 7: Hydrochemical samples: total and processed

Samples	Total	Processed
dissolved oxygen	68	50
nutrients	68	68
suspended matter		

The comparison of the data on dissolved oxygen concentration, measured following the Winkler method and SBE-43 sensor data shown in Figure 27, revealed that for most stations the SBE-43 sensor gave an adequate reflection of the vertical profile although the values were

generally lower. At some stations, the sensor-based concentrations of dissolved oxygen concentrations were higher than the point measurements with the Winkler method.

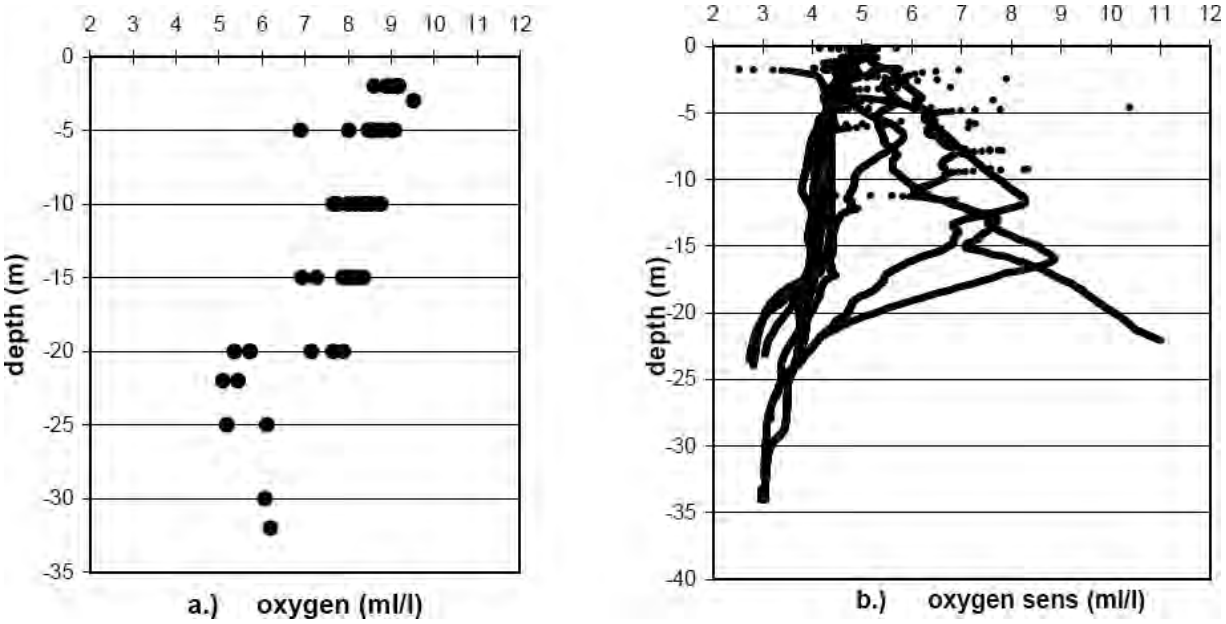

Fig. 27: Vertical distribution of dissolved oxygen measured with the Winkler method (a) and a SBE-43 sensor (b).

The measured concentrations of of dissolved oxygen ranged from 5.09 ml/l (near-bottom water layer, station 8) to 9.52 ml/l (3-m water depth, station 1). The dissolved oxygen concentrations measured by both methods were averaged for all stations at water depths of 2, 5, 10, 15, 20, 22, 25, and 30 m. At almost all water depths sensor values were found to be 1.3-2 times lower than the values obtained by the Winkler method (Fig. 28). The average correction factor is 1.58. In 2008, the average correction factor was 1.56 and ranged from 1.47 to 1.71.

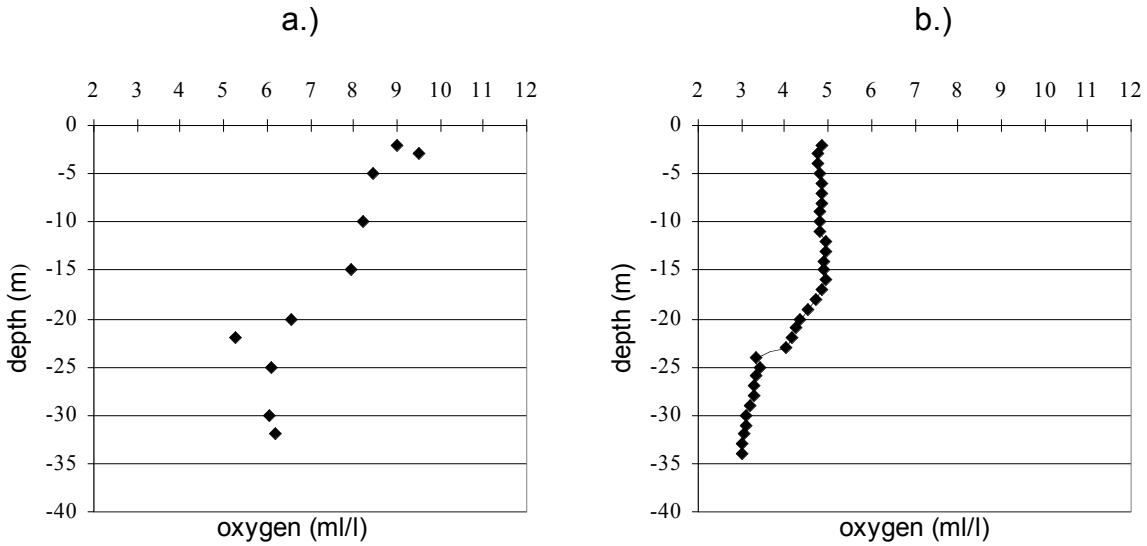

Fig. 28: Averaged for all stations dissolved oxygen concentration measured with Winkler method (a) and SBE-43 sensor (b).

During a later checkup of the oxygen sensor in the calibration laboratory of the producer (Seabird) it was found that the membrane in the CTD was damaged. This damage caused a

strong shift of the sensor data after some measurements. This strong shift of the sensor was already observed during earlier expeditions but it was not detected during the routine maintenance by Seabird before the TRANSDRIFT XV expedition.

In order to compare the vertical distribution of dissolved oxygen in the polynya region of 2008 (TRANSDRIFT XIII) and 2009 (TRANSDRIFT XV), stations from the same polynya region were selected (Fig. 29) and the averaged oxygen concentration plotted (Fig. 30).

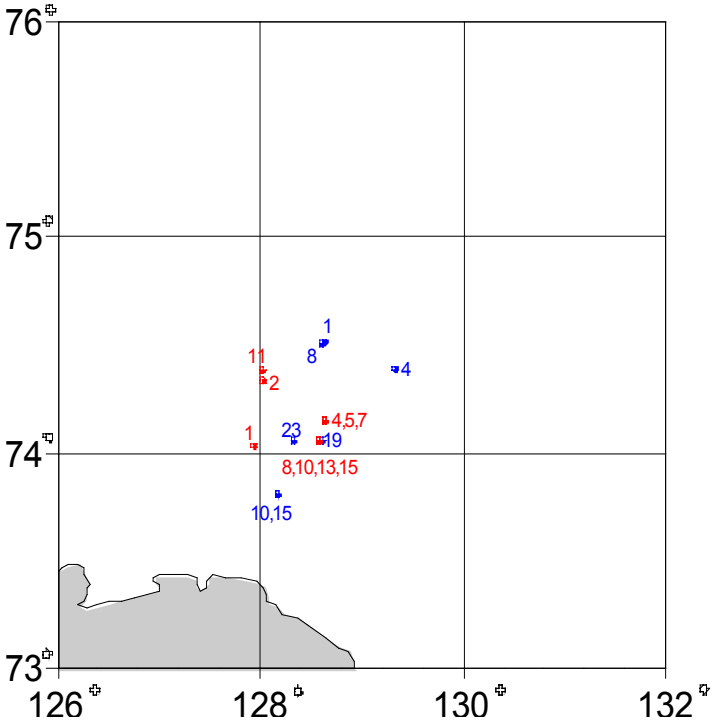

Fig. 29: Water sampling sites selected for plotting the averaged vertical profiles of dissolved oxygen concentration.

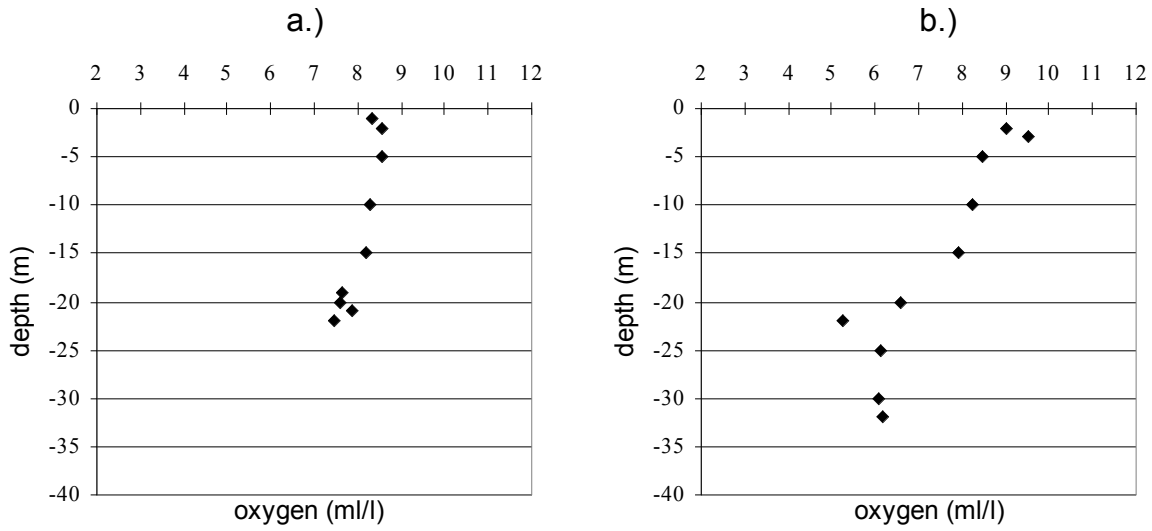

Fig. 30: Vertical profiles of dissolved oxygen concentration measured with Winkler method averaged for selected stations (see Fig. 4): a. TRANSDRIFT XIII (2008), b. TRANSDRIFT XV (2009).

A comparison of both years revealed that in 2009, the surface water layer showed higher concentrations of dissolved oxygen (by 0.5-1 mg/l). This might be due to an enhanced outflow of

oxygen-rich river waters and an earlier phytoplankton bloom than in 2008 (Fig. 30). In the pycnocline the values are almost identical for the two years whereas in the bottom water the values observed in 2009 are by 1-2 ml/l lower than in 2008. This seems to be the result of a weak water stratification in 2008 making possible a deeper downward mixing of oxygen-rich surface waters.

The preliminary data on the concentration of nutrients show the following ranges: silicates from 17.18 µmol/l (5-m water depth, station 1) to 102.4 µmol /l (2 m water depth, station 10); phosphates 0.3 µmol /l (2 m water depth, station 10) to 1.02 µmol /l (22 m water depth, station 8); nitrates from 1.04 µmol /l (5 m water depth, station 1) to 6.61 µmol /l (22m water depth, station 10) (Fig. 31).

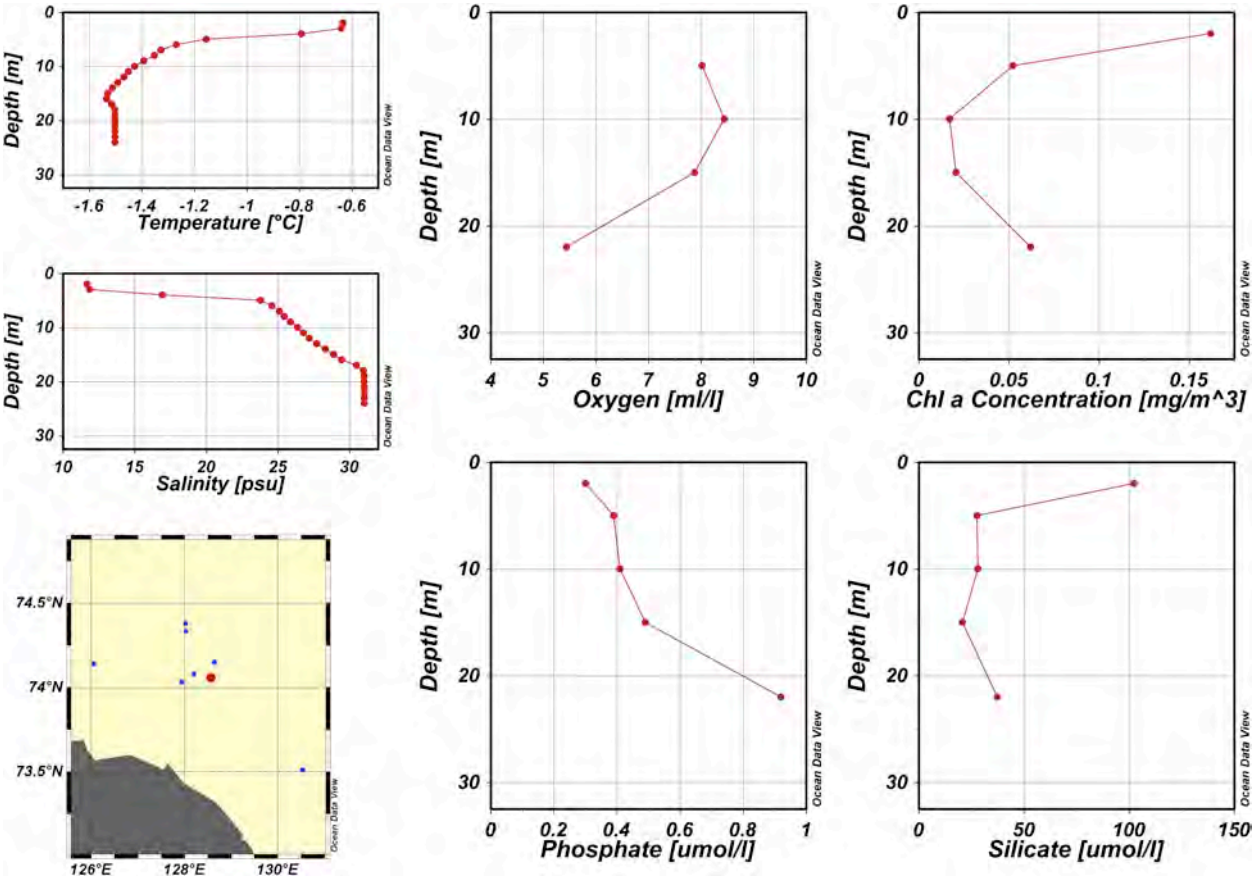

Fig. 31: Oxygen (ml/l), phosphate (µmol/l), silicate (µmol/l) and chlorophyll *a* (mg/m^3) concentration at station TI09-10 on April 14, 2009 (red dot on the map). The high silicate concentration (>100 µmol/l) at the surface points to a fluvial origin of the approx. 3 m thick low salinity layer (<15 psu) under the ice.

5. Ice physics investigations

K. Tyshko
Arctic and Antarctic Research Institute, St. Petersburg, Russia

5.1. Introduction

Investigations of the ice crystal structure, and physical and mechanical properties of sea ice in the Laptev Sea nearshore area, carried out during previous joint Russian-German expeditions, revealed specific stages in sea ice cover formation dependent on the hydrometeorological regime of the basin. Ice crystal structure is highly variable in this area due to changeable dynamic conditions during sea ice freeze-up, such as variability of currents of different velocity and direction together with sharp temperature and salinity oscillations. In the southern Laptev Sea, the structure, and physical and mechanical properties of sea ice are strongly affected by freshwater runoff as sea ice of different salinity ranges is formed. Distribution of the freshwater lens in the flaw polynya and beneath the sea ice cover causes overcooling of both the surface water layer (due to heat loss) and the pycnocline layer (due to convection induced by double-diffusion). Intensive mixing of fresh and seawater produces crystals of frazil ice directly in the mixing layer (due to concentration). Frazil ice and shuga can be transported away from their source region for dozens of kilometers, thus affecting the crystal structure and physical characteristics of the pack ice (Tyshko & Kovalev, 2006).

During spring, evident crystal alignment was observed in the basal fast ice layers formed under the influence of steady surface currents. This physical property is characteristic of the sea ice cover in many arctic seas. Crystal optic analysis of the whole ice sequence reveals a stability of surface currents during the whole sea ice freeze-up period (Dmitrenko et al., 2002).

The considerable temporal variability of the structure and the main physical properties of sea ice, observed during spring time, are caused by thermometamorphism resulting from radiational and conductive heating. It is accompanied by the processes of inner and surface sea ice melting, weakening and destruction of ice. Knowledge about the mechanisms of these processes and the timing of ice transformations from one genetic type to another is essential for practical activities with the use of sea ice as a natural platform (Sea Ice, 1997).

During the TRANSDRIFT XV expedition our investigations of these processes were continued. The program of ice physics investigations includes the following research tasks:

- to investigate the role of frazil ice and shuga in the processes of ice freeze-up and formation of its crystal structure during fall-winter and the first half of spring, when ice of both types is intensively formed in the open water of the polynya zone;
- to investigate the development of crystal alignment (C-axes of crystals) under the effect of steady surface currents;
- to describe the spatial variability of ice crystal structure and physical properties of sea ice in dependence to the regionally dominant processes of sea ice formation;
- to reveal regional peculiarities of the temporal variability in the structure and physical properties of sea ice under the influence of the processes of dynamo and thermometamorphism.

5.2. Instruments and methods

Sea ice temperature was measured with an electronic thermometer Checktemp 1 with a resolution of 0.1°C and laboratory mercury thermometers TL-4 with a scale of 0.1°C and an accuracy of 0.05°C. Ice salinity was measured by a WTW instrument Cond 315i/SET with a

resolution of 0.1‰. Ice texture was visually analyzed in the drilled ice cores. For this purpose a vertical plate with a thickness of 1.0-1.5 cm was cut from every core. Analysis included description of textural layers and all inclusions together with their dimensions. The investigations of ice structure were carried out in the cold laboratory in Tiksi using a polarizing table which consisted of two parallel polaroids lighted from below. Vertical and horizontal ice blocks with a size of 12×9×1.0-1.5 cm were cut from various layers of the ice cores, and thin sections were prepared. The thickness of these sections was 2-3 mm as it should not exceed the size of crystals. The sections were placed between the polaroids for making films and prints (Fig. 32).

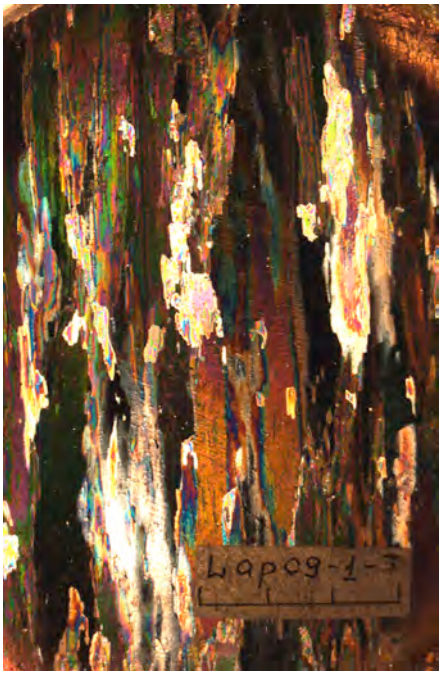

Fig. 32: An example of an ice crystal structure seen under polarized light.

5.3. Main results

As in the previous year, during the 2008-2009 winter season, the sea ice cover near the Laptev Sea flaw polynya developed under intensively dynamic hydrometeorological conditions. The ice thickness in the region of investigation was on average 110-120 cm. This indicates that this fast ice formed at the end of January or early February 2009. During the winter and spring period of fast ice growth, the hydrometeorological conditions were changeable leading to a periodic opening and closure of polynya. The event when the growth of oriented fibrous ice crystals typical for the fast ice (shown in Fig. 32) stopped, and new ice crystals started to grow (Fig. 33) is well expressed in the ice structure. Unlike 2008, such ice movements occurred under generally stable conditions of ice formation in the polynya. This is proved by the presence of thin ice interlayers with isometric structure typical for the periods of sea ice cover growth when the crystals of snow, shuga and frazil ice adfreeze to each other.

As in 2008, ice floes experienced periodical compression under dynamic influence. This resulted in metamorphic transformations of ice crystals and formation of pressure ridges and rafted or layered ice. At compression strength of less than 40% of its critical value (i.e., when ice is crushed) the ice crystals were subject to plastic deformation. The ice crystals started to move along each other thus producing a wavy structure (Fig. 34). When compression strength reached 50-70% of its critical value, the intergranular destruction of ice crystals started (Fig. 35) leading to their complete destruction (Fig. 36). The structure of layers which underwent

maximum compression exceeding 70% of the critical value represented a mass of very small crystal pieces without any expressed edges (Fig. 37) (Tyshko, 2007).

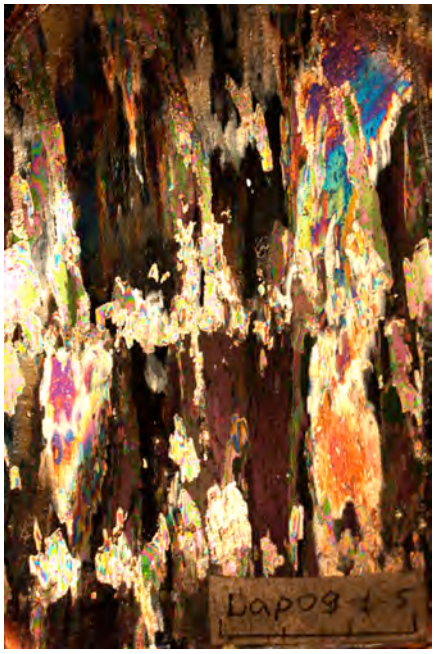

Fig. 33: Layered sea ice structure.

Fig. 34: Plastic intergranular deformation of ice crystals.

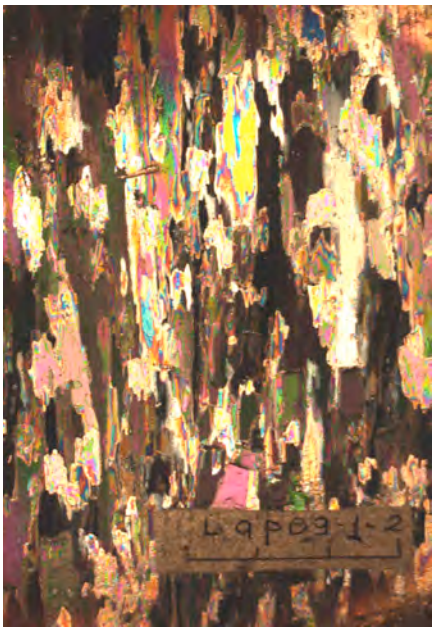

Fig. 35: Intergranular destruction of ice crystals.

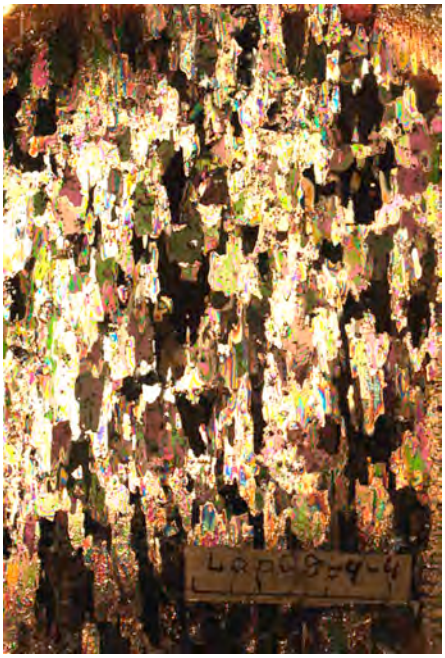

Fig. 36: Onset of the fragile destruction of ice crystals with formation of shapeless groups of very small pieces.

The results of ice physics investigations partly support the data obtained during previous expeditions, but also demonstrate variability in ice structure resulting from different hydrometeorological conditions during the freeze-up period. Similar to 2008, due to extremely active ice freeze-up conditions only at two stations, we observed a clearly expressed alignment of the C-axes of crystals (Fig. 38) typical for many arctic seas with steady surface currents (Sea Ice, 1997). This situation, which is characteristic of the last two years, drastically differs from the more stable situation in 1999 when crystal alignment developed in almost all studied ice cores (Dmitrenko et al., 2002).

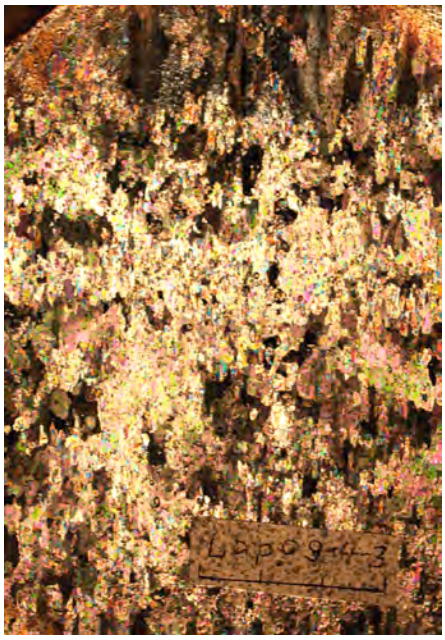

Fig. 37: Intensive fragile destruction of ice crystals with formation of shapeless groups of very small pieces.

Fig. 38: Spatial alignment of crystals on a horizontal ice section.

The most evident difference in the physical properties of sea ice between this and previous years is the low ice salinity, which does not exceed 2‰. This is a result of a considerably lower surface water salinity compared to the average multiannual values. The main reason for the observed freshening is an unusually strong freshwater outflow, which reached the polynya region. The vertical sea ice salinity profile shows two major patterns (Fig. 39). In winter, thevertical salinity profile is characterized by a steady gradual salinity decrease (Fig. 39a). With the onset of radiational heating this physical parameter of sea ice becomes more even in the lower ice layers (Fig. 39b).

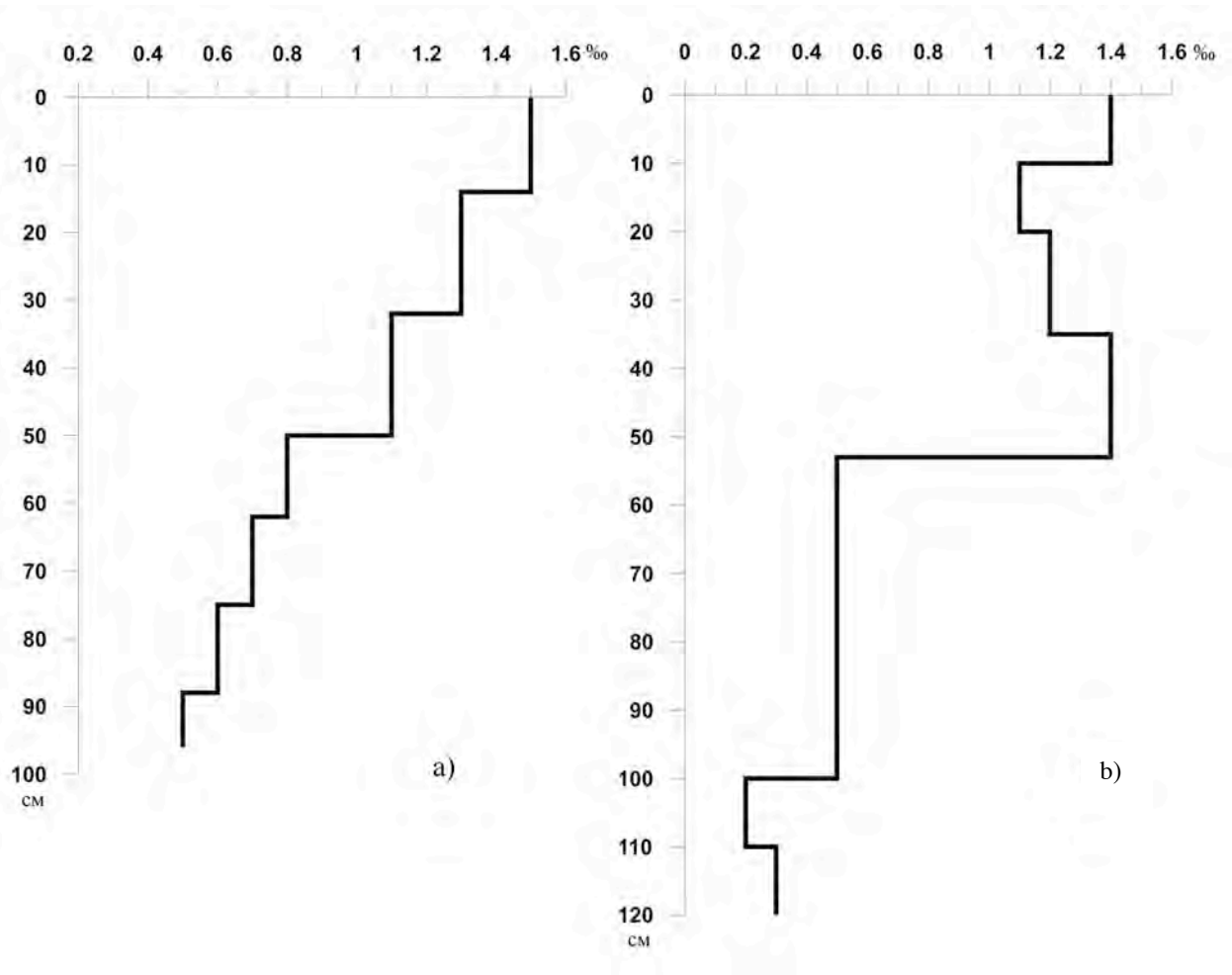

Fig. 39: Typical vertical sea ice salinity profiles measured during the expedition.

The observed considerable freshening of sea ice affected the intensity of radiational heating. In the region under study the sea ice rather remained in the winter-like physical state (Sea Ice, 1997), i.e., it was still relatively fast growing. The number of brine cells in the ice, which are the main accumulators of solar radiation, was low. Therefore the proportion of liquid phase in the ice was not high enough to set on an intensive flow and modify the sea ice texture. Under a relatively low air temperature the sea ice was continuously growing. Due to this, radiational heating was not able to warm the basal ice layer above the surface water temperature as was frequently recorded from previous expeditions (Tyshko & Kovalev, 2005).

6. Biological investigations

E. Abramova[1], F. Martynov[2], D. Taborskii[2], A. Gukov[1], M. Makhotin[3]
[1]State Lena Delta Reserve, Tiksi, Russia
[2]St. Petersburg State University, Russia
[3]Arctic and Antarctic Research Institute, St. Petersburg, Russia

6.1. Introduction

Biological monitoring has been carried out in different parts of the Laptev Sea shelf during the last two decades. The main purpose of these investigations is to reveal the major features of the seasonal cycle and interannual variability of arctic communities based on multiannual observations. The analysis of long-term data series allows establishing certain trends and oscillations in the species composition and dynamics of arctic ecosystems.

It is known that the polynyas on the shelves as large open areas of water in ice-covered regions may be of considerable importance for the overall fixation, cycling, and storage of carbon in the Arctic marine ecosystem since primary and secondary production may increase in ice-free regions (Smith, 1995). Polynyas are particularly sensitive to changes in oceanic and atmospheric forcing. The effect of warming on polynyas affects all elements of the marine ecosystem including benthic and pelagic processes as well as biochemical cycling and its rate. Therefore, polynya dynamics in the Arctic can markedly alter both the productivity and food web structure of high latitude marine environments (Arrigo & van Dijken, 2004). Little is known about the processes regulating population dynamics and community structure of the Arctic marine organisms, but winter mortality is believed to be one potentially important structuring factor (Bagøien et al., 2001).

The main aim of biological investigations during the TRANSDRIFT XV expedition, similar to the previous TRANSDRIFT XIII expedition, was to collect data on the structure of food webs and productivity of Arctic marine ecosystems, both under the fast ice cover and in the open waters of its polynya; and to understand how coexisting different Arctic populations respond numerically and behaviourally to environmental variations during a late winter/spring situation.

The research tasks can be formulated as follows:

- to study spatial and seasonal variations in the species composition, abundance and biomass distribution of phytoplankton, as well as primary production in the polynya region as depending on the light and ice regimes, salinity and temperature conditions, water stratification and concentration of nutrients in April/May 2009;
- to investigate the distribution pattern and seasonal variability of species composition, total abundance and biomass of pelagic, benthic and ice fauna in relation to primary productivity and the hydrological and hydrochemical regimes in the two different years.

6.2. Material

For chlorophyll *a* measurements we collected 67 water samples and 33 ice samples. Water (1 liter) was taken with Niskin bottles in each standard horizon at 13 stations. Ice (upper, middle and lower 10 cm from 11 ice cores) was melted in the dark laboratory at a temperature not above 10°C. All samples were filtered through the glass microfibre filters (GFF) and frozen at -20°C for preservation.

For phytoplankton investigation we collected 68 water samples (1 liter taken with Niskin bottles) from standard horizons at 13 stations; 68 ice samples (upper, middle and lower

10 cm) from 8 ice cores, and 13 net catches (opening diameter 20 cm, mesh size 20 µm). The ice was melted at a temperature not above 4°C. All samples were fixed with 4% neutral formalin.

For zooplankton investigation we collected 25 net catches (opening diameter 20 cm, mesh size 100 µm). At each station net catches were made in the whole water column. Samples were fixed with 4% neutral formalin.

For sea ice fauna investigation we collected 36 ice samples. The ice cores were sawn into blocks: the lower 10 cm into 2 cm thick slices, and the remaining parts of the cores into 10 cm thick ones. The ice samples were melted in excess of filtered seawater and fixed with 4% neutral formalin.

For macrobenthos investigation bottom sediment samples were collected at 8 stations with a Van Veen grab sampler (coverage 250 cm^2). Sampling was carried out from the fast ice edge as well as through a hole in the ice. Benthos was fixed with 70% ethanol.

Chlorophyll *a* measurements and processing of samples for zooplankton and ice fauna study were carried out in the OSL (AARI, St. Petersburg). Phytoplankton samples were analyzed in the Moscow State University, and macrobenthos was analyzed in the State Lena Delta Reserve (Tiksi).

6.3 Preliminary results

6.3.1. Chlorophyll *a* concentration in water

Chlorophyll *a* concentration values in the water column are very low and range from 0.009 mg/m^3 (TI09-09 at 15 m water depth) to 0.1908 mg/m^3 (TI09-13 at 2 m water depth). The highest values are observed in the upper water layers (2-3 m) and average 0.11 mg/m^3, with the maximum value of 0.1908 mg/m^3 recorded at station TI09-13 (2 m water depth), and the minimum value of 0.0558 mg/m^3 recorded at stations TI09-03 and TI09-09 (2 and 3 m water depth, respectively) (Fig. 40). The mean values of chlorophyll *a* concentration at other layers fit the range of 0.03-0.045 mg/m^3.

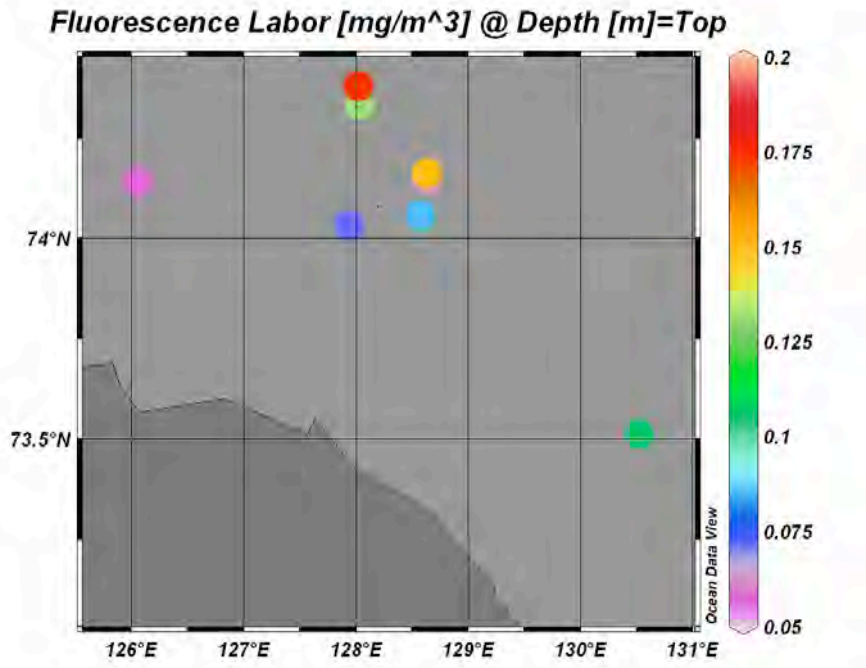

Fig. 40: Concentration of chlorophyll *a* (mg/m^3) in the upper (2-3 m) layer of water column in March-April 2009, TRANSDRIFT XV.

In April-May 2008 (TRANSDRIFT XIII), the highest concentration of chlorophyll *a* was also observed in the upper 5-m thick water layer. The pigment in this layer is distributed unevenly with concentrations ranging from 0.05 to 1.37 mg/m^3 at different stations. Chlorophyll *a* concentration increased in late April/early May due to algae bloom.

To measure the chlorophyll *a* concentration in the water column also the sensor was used which was attached to the SBE19 probe. An analysis of the sensor record with the concentrations measured in the laboratory showed the correlation coefficient between the two curves to be rather high. However, sensor data are on average 3-4 times higher than the values obtained by filter processing.

6.3.2. Chlorophyll *a* concentration in ice

The chlorophyll *a* concentration in the ice cores varies in a very wide range from 17.194 mg/m^3 in the basal layer (0-10 cm) at station TI09-11 to almost zero (0.0065 mg/m^3) in the layer of 80-90 cm at station TI09-02. High values were recorded on March 26 in the basal 10 cm of ice at stations TI09-02 and TI09-03 (3.128 and 4.642 mg/m^3, respectively), and the highest values were observed on April 14 also in the basal 10 cm of ice at stations TI09-09 and TI09-11 (11.844 and 17.194 mg/m^3, respectively) (Fig. 41). Like in April-May 2008 (TRANSDRIFT XIII), the ice samples are enriched in chlorophyll *a* in comparison to the water samples.

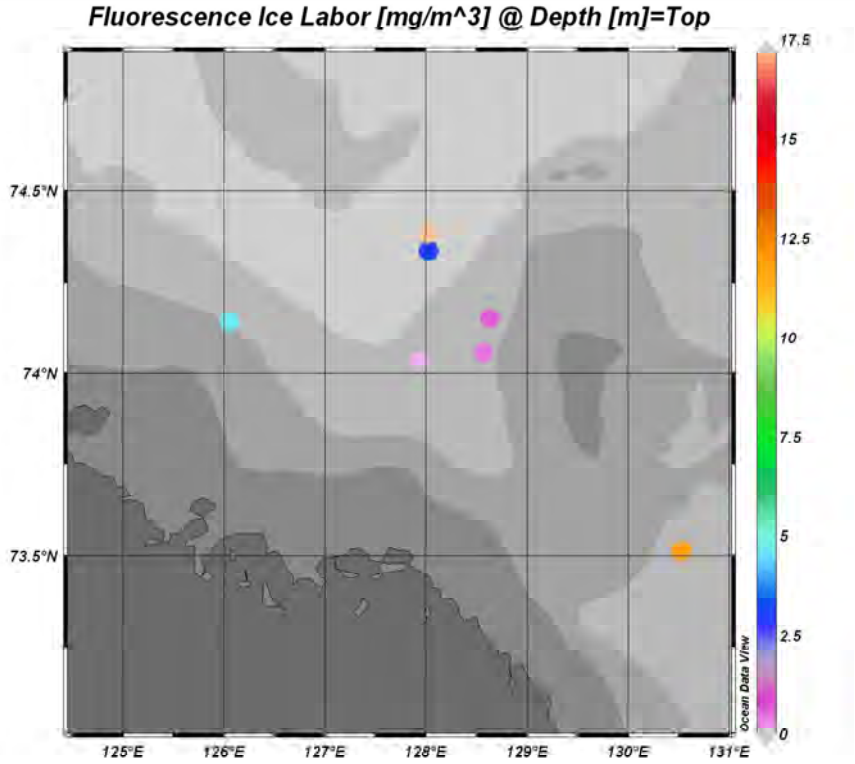

Fig. 41: Concentration of chlorophyll *a* (mg/m^3) in the bottom (0-10 cm) layer of ice in March-April 2009, TRANSDRIFT XV.

The chlorophyll *a* concentration in the basal ice layer (0-10 cm) at other stations was low and varied from 0.025 mg/m^3 (TI09-01) to 0.576 mg/m^3 (TI09-05). The average values for the other layers of the ice cores were very low and ranged between 0.0065 mg/m^3 (TI09-05, layer 110-120 cm) and 0.2124 mg/m^3 (TI09-09, layer 160-170 cm). Therefore, the chlorophyll *a*

concentration in the ice cores shows an evident decrease in the layers above the basal layer (0-10 cm) (Fig. 42).

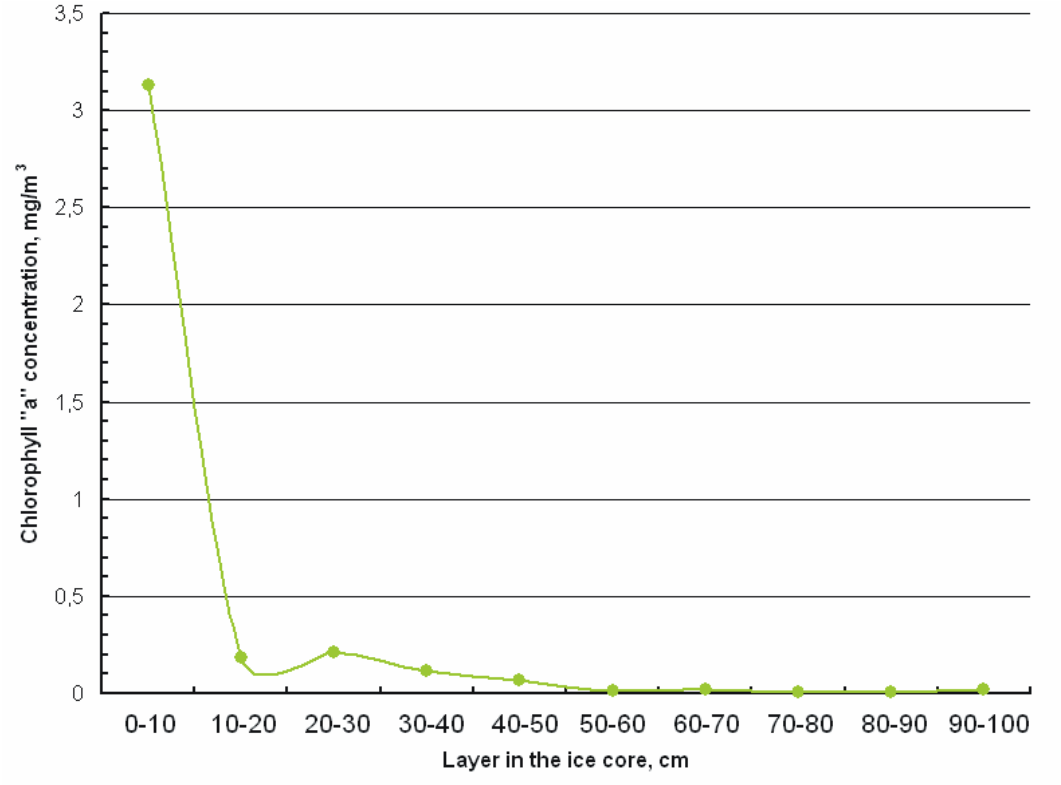

Fig. 42: Downcore concentration of chlorophyll *a* (mg/m^3) in the ice at station TI09-02.

The highest values of chlorophyll *a* concentration in the basal 10 cm of ice at stations TI09-09 and TI09-11, observed on April 14, might be explained by the spring increase in the inflow of nutrient-rich Lena River runoff waters and the development of ice phytoplankton associations on the bottom of the ice.

6.3.3. Zooplankton

Similar to April-May 2008, in March-April 2009 zooplankton was found to be represented by 20 taxa, 10 of which were different Copepoda. The average total abundance of pelagic fauna in 2009 was slightly higher than in the previous year and reached 1580 ind./m^3. It was generally less variable than in 2008 and ranged between 1,112 ind./m^3 and 2,105 ind./m^3.

Copepoda predominate on the Laptev Sea shelf in different seasons. During the period of investigations they formed two ecologically different assemblages. The first assemblage was represented by marine euryhaline species including *Oithona similis*, *Microcalanus pigmaeus*, *Oncaea borealis, Microcetella norvegica* and *Calanus* spp. The second assemblage largely consisted of brackish-water neritic species, such as *Pseudocalanus* spp., *Drepanopus bungei*, *Acartia longiremis*, and *Limnocalanus macrurus.* In 2009, as in 2008, *O. similis* and *M. pigmaeus* were dominant among marine species. In 2008, the average relative abundance of *O. similis* reached 20% of the total zooplankton abundance, but in 2009 it dropped down to 9%. On the contrary, the relative abundance of *M. pigmaeus* slightly increased from 7.5% in 2008 to 10% in 2009. At the same time, in 2009 the relative percentage of brackish-water Copepoda of the Pseudocalanidae family increased and the share of *Pseudocalanus* spp. and *D. bungei* reached 11% and 7%, respectively. The relative representation of *A. longiremis* did not change during both years and remained close to 7%. Unlike 2008, when marine Copepoda

predominated at all stations, in 2009 both ecological groups were equally abundant. Copepod nauplii were the most abundant organisms in the planktic fauna during both years, and their average percentage reached 46% of the total zooplankton abundance in 2008 and 50% in 2009 (Fig. 43). Among the remaining planktic organisms juvenile Polychaeta and Scyphozoa were the most abundant.

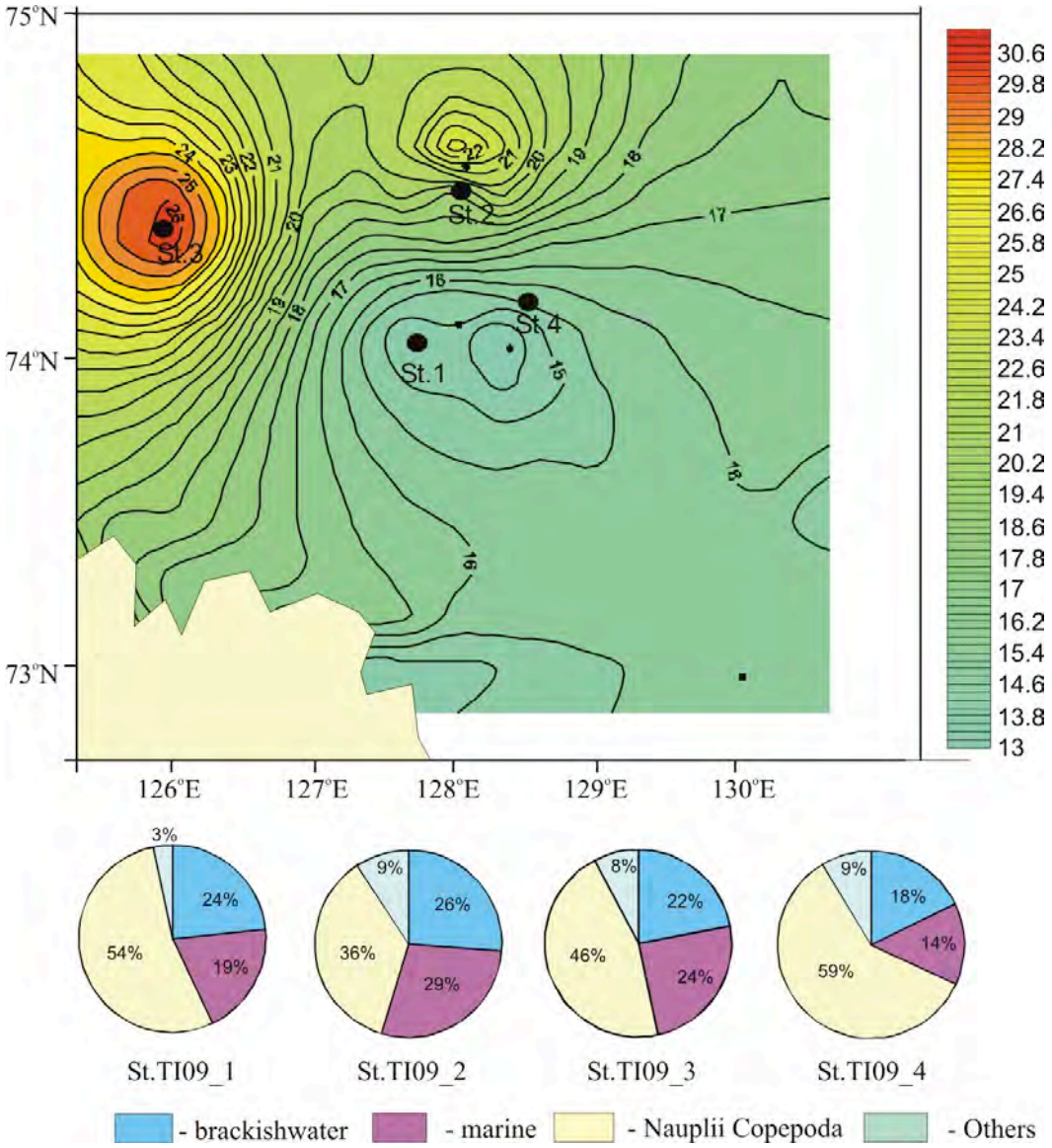

Fig. 43: Salinity distribution and relative abundance of common ecological groups of zooplankton in the Laptev Sea polynya in March-April 2009.

The average multiannual data show that the brackish-water species *Pseudocalanus major*, *P. acuspes* and *D. bungei* are constantly present among the dominant zooplankton assemblage on the Laptev Sea shelf (Abramova & Tuschling, 2005). In April-May 2008, salinity in the region of our investigations was relatively high even in the surface layer (up to 30‰). This is a result of the summer 2007 hydrological development when the river water plume was largely shifted eastward and left the Laptev Sea via the straits between the New Siberian Islands. Thus, in summer 2007 the brackish-water plankton, which is usually restricted to the freshened regions of the Laptev Sea, was rare in the inner Laptev Sea shelf. This situation continued in the winter of 2008. In March-April 2009, surface water salinity was close to the average multiannual values and even less. Correspondingly, the composition of the pelagic

fauna in the region under study changed, and the relative abundance of brackish-water organisms increased (Fig. 43).

The age-sex structure of the populations of *O. similis* and *Pseudocalanus* spp., the species which are dominant in the polynya region, is very similar throughout the region of investigations (Fig. 44A). Adult females predominate in the population of *O. similis* including rare females with spermatophores and egg sucks. The presence of early copepodite stages indicates that this species was reproducing during late winter 2009. The population of brackish-water *Pseudocalanus* spp. is dominated by the overwintered III-V copepodite stages. Also, some adult males and females are present as well as representatives of I-II stages of the new generation (Fig. 44B), thus evidencing the beginning of reproduction of this species.

Samples of phytoplankton, macrozoobenthos, meiobenthos, and ice fauna collected during the TRANSDRIFT XV expedition are currently being processed and are stored in the OSL (AARI, St. Petersburg).

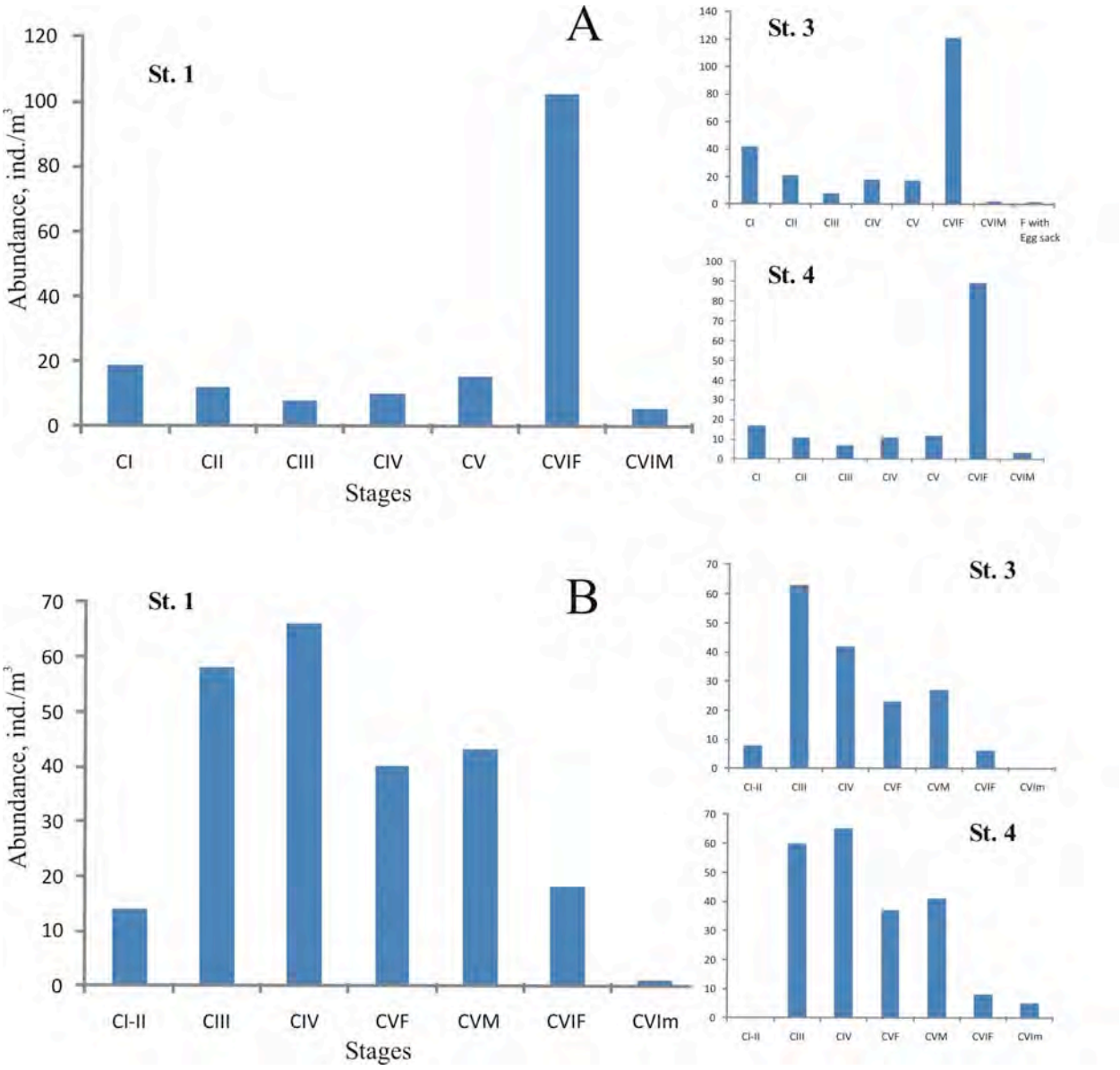

Fig. 44: Age structure of copepodite stages in populations of *Oithona similis* (A) and *Pseudocalanus* spp. (B) in the Laptev Sea polynya region during winter 2009.

6.4. Preliminary conclusions

The hydrological situation in the Laptev Sea polynya region was strongly different in March-April 2009 (TRANSDRIFT XV) and April-May 2008 (TRANSDRIFT XIII). This difference was reflected in various components of the local ecosystem. A clear relationship was recorded between the relative abundance of ecologically different groups of Copepoda species and the salinity regime. At the same time, chlorophyll *a* concentration in water and ice, determined during the two years, do not differ considerably. However, it should be mentioned that in 2009 the investigations were made during the second half of March and April, i.e., the time of the onset of phytoplankton bloom. The observed higher concentrations of nutrients already during this period compared to April-May 2008 allow assuming that chlorophyll *a* concentrations should have further increased in the region under study by early May 2009 due to extensive phytoplankton bloom.

REFERENCES

Abramova, E., and Tuschling, K. (2005) A 12-year study of the seasonal and interannual dynamics of mesozooplankton in the Laptev Sea: significance of salinity regime and life cycle patterns. Global and Planetary Change, Special Issue, 48(1-3): pp. 141-164. doi: 10.1016/j.gloplacha.2004.12.010.

Arctic Climate Impact Assessment (ACIA) (2004) Cambridge: Cambridge University Press, CB2 2RU, UK, 2004.

Arrigo, K.R. and van Dijken, G.L. (2004) Annual cycles of sea ice and phytoplankton near Cape Bathurst, southeastern Beaufort Sea, Canadian Arctic. Geophysical Research Letters, 31(8): L08304, doi:10.1029/2003GL018978.

Bagøien, E., Kaartvedt, S., Aksnes, D.L., and Eiane, K. (2001) Vertical distribution and mortality of overwintering *Calanus*. Limnology and Oceanography, 46: pp. 1494-1510.

Dmitrenko, I.A., Tyshko, K.P., Hoelemann, J.A., Eicken, H., and Kassens, H. (2002) Water circulation and crystal structure of sea ice in the marginal area of the laptev Sea flaw polynya. Meteorology and Hydrology, 8: pp. 67-76 (in Russian).

Drucker, R., Martin, S., and Moritz, R. (2003) Observation of ice thickness and frazil ice in the St. Lawrence Island polynya from satellite imagery, upward looking sonar, and salinity/temperature moorings. Journal of Geophysical Research, 108(C5): doi:10.1029/ 2001JC001213.

Haas, C. (2004) Late-summer sea ice thickness variability in the Arctic Transpolar Drift 1991-2001 derived from ground-based electromagnetic sounding. Geophysical Research Letters, 31: L09402, doi:10.1029/2003GL019394.

Johannessen, O.M., Miles, M., and Bjorgo, E. (1995) The Arctic's shrinking sea ice. Nature, 376: pp. 126-127.

Kanamitsu, M., Ebisuzaki, W., Woollen, J., Yang, S.-K., Hnilo, J.J., Fiorino, M., and Potter, G.L. (2002) NCEP-DEO AMIP-II Reanalysis (R-2). Bulletin of American Meteorological Society, 1631-1643.

Key, J.R., Collins, J.B., Fowler, C., and Stone, R.S. (1997) High-latitude surface temperature estimates from thermal satellite data. Remote Sensing of Environment, 61: pp. 302-309.

Kirillov, S.A., Makhotin, M., and Dmitrenko, I.A. (2009) The Siberian shelves thermohaline structure: the long-term climatic changes and their causes. In: Kassens, H., Lisitzin, A.P., Thiede, J., Polyakova, Y.I., Timokhov, L.A., and Frolov, I.E. (eds.). Climate changes of the Siberian shelf waters thermohaline structure and their causes. Moscow: MSU Press, pp. 173-186 (in Russian).

Maslanik, J.A., Serreze, M.C., and Barry, R.G. (1996) Recent decreases in Arctic summer ice cover and linkages to atmospheric circulation anomalies. Geophysical Research Letters, 23: pp. 1677-1680.

Polyakov, I., Beszczynska, A., Carmack, E., Dmitrenko, I., Fahrbach, E., Frolov, I., Gerdes, R., Hansen, E., Holfort, J., Ivanov, V., Johnson, M., Karcher, M., Kauker, F., Morison, J., Orvik, K., Schauer, U., Simmons, H., Skagseth, O., Sokolov, V., Steele, M., Timokhov, L., Walsh, D., and Walsh, J. (2005) One more step toward a warmer Arctic. Geophysical Research Letters, 32: doi:10.1029/2005GL023740.

Polyakov, I.V., Alexeev, G.V., Timokhov, L.A., Bhatt, U.S, Colony, R.L., Simmons, H.L., Walsh, D., Walsh, J.E., and Zakharov, V.F. (2004) Variability of the intermediate Atlantic Water of the Arctic Ocean over the last 100 years. Journal of climate, 17(23): pp. 4485-4497.

Rothrock, D.A., Yu, Y., and Maykut, G.A. (1999):Thinning of the Arctic sea-ice cover. Geophysical Research Letters, 26: pp. 3469-3472.

Sea Ice. Collection and analysis of observational data, physical properties, and forecast of ice conditions (reference materials) (1997) St. Petersburg: Gidrometeoizdat, 402 pp. (in Russian).

Smith, W.O. Jr. (1995) Primary productivity and new production in the Northeast Water (Greenland) Polynya during summer 1992. Journal of Geophysical Research, 100: pp. 4357-4370.

Tyshko, K.P. (2007) Structural classification of dynamomethamorphic modifications of one-year sea ice. Meteorology and Hydrology, 8: pp. 69-76 (in Russian).

Tyshko, K.P. and Kovalev, S.M. (2005) Temperature regime of the arctic sea ice cover in mid-spring. Meteorology and Hydrology, 6: pp. 92-102 (in Russian).

Tyshko, K.P. and Kovalev, S.M. (2006) The role of water-shuga layers in the growth of one-year ice and consolidation of pressure ridges. Meteorology and Hydrology, 8: pp. 72-82 (in Russian).

Yu, Y. and Rothrock, D.A. (1996) Thin ice thickness from satellite thermal imagery. Journal of Geophysical Research, 101(C10): pp. 25,753-25,766.

Yu, Y. and Lindsay, R.W. (2003) Comparison of thin ice thickness distributions derived from RADARSAT Geophysical Processor System and advanced very high resolution radiometer data sets. Journal of Geophysical Research, 108(C12):pp. doi:10.1029/2002JC001319.

APPENDIX

List of participants
Station list

List of participants

No.	Name	Affiliation
1	Abramova, Ekaterina	State Lena Delta Reserve, Tiksi
2	Adams, Susanne	Trier University
3	Bloshkina, Ekaterina	AARI, St. Petersburg
4	Dmitrenko, Igor	IFM-GEOMAR, Kiel
5	Doering, Uwe	Ministry of Justice, Labor and European Affairs, Kiel
6	Esipenko, Sergey	State Hydrometeorological Department, Tiksi
7	Ezhikov, Sergey	State Hydrometeorological Department, Tiksi
8	Gukov, Alexander	State Lena Delta Reserve, Tiksi
9	Helbig, Alfred	Trier University
10	Hoelemann, Jens	AWI, Bremerhaven
11	Kassens, Heidemarie	IFM-GEOMAR, Kiel
12	Kirillov, Sergey	IFM-GEOMAR, Kiel
13	Klagge, Torben	IFM-GEOMAR, Kiel
14	Krumpen, Thomas	AWI, Bremerhaven
15	Makhotin, Mikhail	AARI, St. Petersburg
16	Martynov, Fedor	St. Petersburg State University
17	Semenov, Vladimir	State Hydrometeorological Department, Tiksi
18	Taldenkova, Ekaterina	Moscow State University
19	Tyshko, Konstantin	AARI, St. Petersburg
20	Vizitov, Viktor	AARI, St. Petersburg

TRANSDRIFT XV

Station #	Date	Time (Tiksi)	Latitude (° N)	Longitude (° E)	Depth (m)	Activity	Ice thickness	Wind / temperature	Notes
TI 09 01	24.03.09	11:20	74°01.995'	127°56.0928'	26,1	begin of station	100 cm	S, 1 m/s, -25°C	Camp: POLYNYA I
-1		12:07				CTD with sensors for turbidity, oxygen, chlorophyll A			
-2		12:30				water sampling for oxygen, chlorophyll, nutrients, phytoplankton			
-3		14:05				net			18 cm diameter; 100 μm
-4		16:20				net			18 cm diameter; 20 μm
-5		16:30				ice core (9 cm diameter): ice biology			2 cores
-6		16:40				mooring (4 CTD, 1 ADCP 300 kHz)			microcats 6723: 1,5m, 6726: 8m; 6752: 15m, 6724: 25m, ADCP LAVAL: 2m
						deployment meteorological station "red"			
-7		14:00				ice physics			2 ice cores, temperature, salinity, texture
		13:55 - 14:49				photo profile sea-ice thickness			
		15:30				end of station			
TI 09 02	26.03.09	13:50	74°20.068'	128°01.643'	32,6	begin of station	95 cm	SW, 5-6 m/s, -14°C	Station ANABAR
-1		14:03				CTD with sensors for turbidity, oxygen, chlorophyll A			
-2		14:05				water sampling for oxygen, chlorophyll, nutrients, phytoplankton			2, 5, 10, 15, 20, 25, 30 m
-3		15:12				net			18 cm diameter; 100 μm
-4						net			18 cm diameter; 20 μm
-5						ice core (9 cm diameter): ice biology			2 cores
-6		14:00				ice physics			2 ice cores, temperature, salinity, texture
-7		14:30				mini box core			
		15:20				end of station			
TI 09 03	26.03.09	16:17	74°08,459'	126°03,418'		begin of station	33 cm	SW, 3 m/s, -14°C	
-1		16:32			17,1	CTD with sensors for turbidity, oxygen, chlorophyll A			
-2		16:35				water sampling for oxygen, chlorophyll, nutrients, phytoplankton			2, 5, 10, 15 m
-3		17:10				net			
-4		16:30				ice physics			
-5		17:00				mini box core			
		17:13 - 18:00				photo profile sea-ice thickness			
		18:00				end of station			
TI 09 04	27.03.09		74°09,086'	128°38,043		begin of station			Camp POLYNYA II
-1						ice physics; 1 ice core			
-2						Meteorological station No 2 deployed			
-3						Biology benthos sampling (snapper)			
-4		13:20			22,6	CTD with sensors for turbidity, oxygen, chlorophyll A			
-5						ice core (9 cm diameter): ice biology - fauna			
-6						water sampling for oxygen, chlorophyll, nutrients, phytoplankton			
-7						net			18 cm diameter; 100 μm
-8						net			18 cm diameter; 20 μm
		15:09 - 15:54				photo profile sea-ice thickness			
-9		13:30				deployment mooring (4 CTD, 1 ADCP 300 kHz)			microcats 1,5 m (6722), 8 (6720), 15 (6721), 20 (6727); ADCP 2 m (7319; AARI)
		16:00				end of station			

TRANSDRIFT XV

Station #		Date	Time (Tiksi)	Latitude (° N)	Longitude (° E)	Depth (m)	Activity	Ice thickness	Wind / temperature	Notes
TI 09 05		01.04.09		74°09,086'	128°38,043'		begin of station		-12°C	Camp POLYNYA II
	-1		12:35				CTD with sensors for turbidity, oxygen, chlorophyll A			
	-2		14:30				water sampling for oxygen, chlorophyll, nutrients, phytoplankton			2, 5, 10, 17 m
	-3		15:10				net			18 cm diameter; 100 μm
	-4						net			18 cm diameter; 20 μm
	-5						ice core (9 cm diameter): ice biology			3 cores
	-6		15:30				deployment mooring (2 CTD, 1 ADCP 300 kHz)			microcats 3m (5388), 17m (1604); ADCP 7944: 2m
	-7		14:05	74°40.365	131°14.745		Meteorological station No 3 installation			
	-8						ice physics			2 ice cores, temperature, salinity, texture
	-9		13:50				fishing at the ice edge			
	-10		14:30				Biology benthos sampling (snapper)			
			15:22 - 15:30				photo profile sea-ice thickness			
			15:32 - 15:47				photo profile sea-ice thickness			
			16:32				end of station			
TI 09 06		02.04.09	11:39	74°04.846'	128°11.812'		begin of station			Camp POLYNYA I: recovery
	-1		12:43			25,9	CTD with sensors for turbidity, oxygen, chlorophyll A			2 casts
			13:15				end of station			
TI 09 07		03.04.09	11:43	74°09,08'	128°38,085'		begin of station		2 m/s NW; -19°C	Camp POLYNYA II: recovery
	-1		12:15				CTD with sensors for turbidity, oxygen, chlorophyll A			2 casts
	-2						Biology benthos sampling (8 snapper)			
			14:45				end of station			
TI 09 08		08.04.09	12:30			23,4 m	begin of station	118 cm	6 m/s SE; -9°C	Camp POLYNYA III; 800 m distance from ice edge
	-1		12:56	74°03,311'	128°34,501'		CTD with sensors for turbidity, oxygen, chlorophyll A			2 casts
	-2		13:00				water sampling: oxygen, CHL A, nutrients, phytoplankton			2, 5, 10, 15, 20
	-3		13:10				net			18 cm diameter; 100 μm
	-4						net			18 cm diameter; 20 μm
	-5						ice core (9 cm diameter): ice biology			2 cores
	-6		14:40	74°03,475'	128°33,935'		deployment mooring (4 CTD, 1 ADCP 300 kHz)			microcats: 2m (6726); 8m (6725); 15m (6724); 22m (6723); ADCP Laval 2,5 m
				74°03'311	128°34'501		deployment meteorological station "red"			
			14:33 - 15:21				photo profile sea-ice thickness			
			16:15				end of station			
TI 09 09	-1	14.04.09	12:30	73°30,71'	130°31,567'		deployment meteorological station "blue"		10 m/s S; -24°C	
			13:12				CTD with sensors for turbidity, oxygen, chlorophyll A	155 cm		
			13:15				water sampling: oxygen, CHL A, nutrients, phytoplankton			3, 5, 10, 15, 20, 22
			14:20				end of station			
TI 09 10		14.04.09	12:20	74°30,484	128°33,883	23,8			10 m/s S; -23°C	Camp POLYNYA III
	-1						CTD with sensors for turbidity, oxygen, chlorophyll A			fast ice
	-2		12:20	73°48.313	128°09.725		water sampling for oxygen, chlorophyll, nutrients, phytoplankton			2, 5, 10, 15 m
	-3		12:45				ice physics; 2 ice core			65 cm fast ice, temperature, salinity
	-4		13:00				net			40 cm diameter; 55 μm

TRANSDRIFT XV

Station #		Date	Time (Tiksi)	Latitude (° N)	Longitude (° E)	Depth (m)	Activity	Ice thickness	Wind / temperature	Notes
TI 09 10	-5		13:15	73°48.334	128°09.671		Mini box core			new ice
	-6		13:40				net			18 cm diameter; 100 μm
	-7		13:45				net			18 cm diameter; 20 μm
	-8		12:28	73°48.334	128°09.671		CTD			31 cm new ice
	-9		12:36	73°48.365	128°09.562		CTD			26 cm new ice
	-10		12:42	73°48.390	128°09.424		CTD			28 cm new ice
	-11		12:51	73°48.417	128°09.292		CTD			28 cm new ice
	-12		12:59	73°48.456	128°09.183		CTD			30 cm new ice
	-13		13:05	73°48.404	128°09.099		CTD			26 cm new ice
	-14		13:12	73°48.549	128°09.013		CTD			25 cm new ice
	-15		13:42	73°48.086	128°10.236		CTD			68 cm fast ice
	-16		13:49	73°48.146	128°10.124		CTD			68 cm fast ice
	-17		13:56	73°48.203	128°10.019		CTD			68 cm fast ice
	-18		14:05	73°48.265	128°09.890		CTD			60 cm fast ice
	-19		14:10				ice core (9 cm diameter): ice biology and fauna			3 cores
	-20		12:05				Biology benthos sampling (8 snapper)			
			14:25 - 15:02				photo profile sea-ice thickness (Heli 2)			
			15:36 - 16:26				photo profile sea-ice thickness (Heli 2)			
			14:18				end of station			
TI 09 11		15.04.09	13:15				begin of station		12-14 m/s S; -12°C	drifting fast ice 110 cm, N of ANABAR
	-1		14:00	74°24,88'	128°01,223'	33,7	CTD with sensors for turbidity, oxygen, chlorophyll A			
			14:20	74°22,88'	128°01,223'					
	-2		15:45				water sampling for oxygen, chlorophyll, nutrients, phytoplankton			2, 5, 10, 15, 20 ,23 m
	-3		16:10				net			18 cm diameter; 100 μm
	-4						net			18 cm diameter; 20 μm
	-5						ice physics			2 ice cores, temperature, salinity, texture
	-6		15:20				Biology benthos sampling (8 snapper)			
	-7		16:05	73°55.657	127°35.051		CTD			30 cm new ice
	-8		16:12	73°55.609	127°35.231		CTD			30 cm new ice
	-9		16:20	73°55.556	127°35.414		CTD			31 cm new ice
	-10		16:26	73°55.511	127°35.637		CTD			31 cm new ice
	-11						ice core (9 cm diameter): ice biology			2 cores
			14:36 - 15:47				photo profile sea-ice thickness			
			16:52				end of station			
TI 09 12		15.04.09		74°03,484'	128°33,883					Camp POLYNYA III
			16:05	74°03,475'	128°33,935	23,8	CTD with sensors for turbidity, oxygen, chlorophyll A			2 casts
TI 09 13		21.04.09	13:02	74°03,465'	128°33,827'		begin of station	114 cm	10 m/s S; -11°C	Camp POLYNYA III
	-1		13:20	74°03,475'	128°33,935		CTD with sensors for turbidity, oxygen, chlorophyll A			2 casts
	-2						water sampling for oxygen, chlorophyll, nutrients, phytoplankton			2, 5, 10, 15, 18 cm
	-3						net			18 cm diameter; 100 μm
	-4						net			18 cm diameter; 20 μm
	-5						ice core (9 cm diameter): ice biology			2 cores
	-6		13:57	74°40.352	131°14.360		CTD			40 cm new ice

TRANSDRIFT XV

Station #		Date	Time (Tiksi)	Latitude (° N)	Longitude (° E)	Depth (m)	Activity	Ice thickness	Wind / temperature	Notes
TI 09 13	-7		14:05	74°40.359	131°14.079		CTD			37 cm new ice
	-8		14:12	74°40.383	131°13.831		CTD			32 cm new ice
	-9		14:21	74°40.405	131°13.574		CTD			31 cm new ice
	-10		14:46	74°40.354	131°14.686		CTD			140 cm fast ice
	-11		14:57	74°40.357	131°14.825		CTD			145 cm fast ice
	-12						ice physics			125 cm fast ice; salinity, temperature
	-13						ice core for oxygen			72 cm
	-14						Biology benthos sampling (8 snapper)			
			14:27 - 15:00				photo profile sea-ice thickness			
			15:01				end of station			
TI 09 14		21.04.2008	15:21				begin of station	15 - 35 cm	10 m/s S; -11°C	Thin ice calibration
	-1		15:56				water sampling for oxygen, chlorophyll, nutrients, phytoplankton			2, 5, 10, 15,20,25, 28 m
	-2		16:20				net			18 cm diameter; 100 μm
	-3						net			18 cm diameter; 20 μm
	-4						ice core (9 cm diameter): ice biology			2 cores
	-5		16:16	74°36.092	130°43.808		CTD			35 cm new ice
	-6		16:26	74°36.121	130°43.556		CTD			30 cm new ice
	-7		16:37	74°36.150	130°43.321		CTD			32 cm new ice
	-8		16:44	74°36.180	130°43.108		CTD			32 cm new ice
	-9						ice physics			2 ice cores, temperature, salinity, texture
	-10						ice core for oxygen			65 cm
	-11						Biology benthos sampling (8 snapper)			
	-12						ice core (9 cm diameter): ice biology			2 cores
			17:30				end of station			
TI 09 15		23.04.09	12:54				begin of station	118 cm	5-7 m/s SE; -14°C	Camp POLYNYA III
				74°03, 311	128°34, 501		recovery meteorological station "red"			
				74°03, 488	128°33, 930		recovery of POLYNYA III			
	-1		13:20	74°03, 475	128°33, 935		CTD with sensors for turbidity, oxygen, chlorophyll A			
	-2		13:12				water sampling for oxygen, chlorophyll, nutrients, phytoplankton			2, 5, 10, 15, 21
	-3		13:30				net			18 cm diameter; 100 μm
	-4						net			18 cm diameter; 20 μm
	-5		13:18	73°48.335	128°09.679		CTD			36 cm new ice
	-6		13:24	73°48.366	128°09.560		CTD			35 cm new ice
	-7		13:34	73°48.548	128°09.005		CTD			32 cm new ice
	-8		13:40	73°48.504	128°09.105		CTD			35 cm new ice
	-9		13:47	73°48.457	128°09.183		CTD			38 cm new ice
	-10		13:52	73°48.417	128°09.289		CTD			39 cm new ce
	-11		14:03	73°48.265	128°09.885		CTD			60 cm fast ice
	-12		14:10	73°48.201	128°10.017		CTD			69 cm fast ice
	-13		14:16	73°48.146	128°10.129		CTD			65 cm fast ice
	-14		14:20	73°48.091	128°10.223		CTD			89 cm fast ice
	-15						Biology benthos sampling (8 snapper)			
	-16						ice core (9 cm diameter): ice biology			2 cores
			14:56				end of station			

TRANSDRIFT XV

Station #	Date	Time (Tiksi)	Latitude (° N)	Longitude (° E)	Depth (m)	Activity	Ice thickness	Wind / temperature	Notes
TI 08 16	23.04.09	15:50				begin of station	180 cm	5-7 m/s SE; -14°C	
						recovery meteorological station "blue"			
-1		16:15	73°30,711'	130°31,567'	24,5	CTD with sensors for turbidity, oxygen, chlorophyll A			
-2		16:20	74°22.6	127°47.013		CTD with sensors for turbidity, oxygen, chlorophyll A			
-3		16:25				water sampling			2,5,10,15,20,25,30
-4		17:00				net			18 cm diameter; 100 μm
-5						net			18 cm diameter; 20 μm
		17:19	74°22.319	127°46.849		GPS position 2			strong drift
-6						Biology benthos sampling (8 snapper)			
-7						ice core (9 cm diameter): ice biology			2 cores
		17:37				end of station			